PLoS GENETICS

A Cholinergic-Regulated Circuit Coordinates the Maintenance and Bi-Stable States of a Sensory-Motor Behavior during *Caenorhabditis elegans* Male Copulation

Yishi Liu[1], Brigitte LeBeouf[1,2], Xiaoyan Guo[1], Paola A. Correa[1], Daisy G. Gualberto[1,2], Robyn Lints[1], L. Rene Garcia[1,2]*

1 Department of Biology, Texas A&M University, College Station, Texas, United States of America, 2 Howard Hughes Medical Institute, Texas A&M University, College Station, Texas, United States of America

Abstract

Penetration of a male copulatory organ into a suitable mate is a conserved and necessary behavioral step for most terrestrial matings; however, the detailed molecular and cellular mechanisms for this distinct social interaction have not been elucidated in any animal. During mating, the *Caenorhabditis elegans* male cloaca is maintained over the hermaphrodite's vulva as he attempts to insert his copulatory spicules. Rhythmic spicule thrusts cease when insertion is sensed. Circuit components consisting of sensory/motor neurons and sex muscles for these steps have been previously identified, but it was unclear how their outputs are integrated to generate a coordinated behavior pattern. Here, we show that cholinergic signaling between the cloacal sensory/motor neurons and the posterior sex muscles sustains genital contact between the sexes. Simultaneously, via gap junctions, signaling from these muscles is transmitted to the spicule muscles, thus coupling repeated spicule thrusts with vulval contact. To transit from rhythmic to sustained muscle contraction during penetration, the SPC sensory-motor neurons integrate the signal of spicule's position in the vulva with inputs from the hook and cloacal sensilla. The UNC-103 K$^+$ channel maintains a high excitability threshold in the circuit, so that sustained spicule muscle contraction is not stimulated by fewer inputs. We demonstrate that coordination of sensory inputs and motor outputs used to initiate, maintain, self-monitor, and complete an innate behavior is accomplished via the coupling of a few circuit components.

Introduction

Male copulation is the most complex behavior for *C. elegans* [1]. The nervous system must integrate sensory cues from the hermaphrodite to generate instructions for each step of mating. In addition, the sex-specific mating circuits monitor the progress, and then determine whether to retain the current motor pattern or to adopt a new action [2]. This is done simultaneously as they convey information to the general locomotion circuit to coordinate the male's movements with the hermaphrodite's [3]. The function of the male's nervous system is also modulated by gender determining factors, nutritional state and the presence of food odors [4–7].

The 302 neurons in *Caenorhabditis elegans* hermaphrodites and the 383 neurons in males encode a variety of general behaviors like feeding, locomotion, defecation and sensory modalities in both sexes. The circuits controlling these behaviors are comprised of a few neurons and muscles that are multifunctional in sensing, processing and commanding signals [8–17]. In contrast to many *C. elegans* hermaphrodite-studied sensory and motor actions, the

male-executed copulation is a multi-component task-orientated behavior. Under an idealized mating situation, the male presses his sensory laden tail firmly on a receptive hermaphrodite, and adjusts his posture so that he laterally scans the dorsal and ventral cuticle of his mate, searching for the vulva. He would then position his tail over the vulva and extend a pair of copulatory spicules from his cloacal opening to pry apart the vulva lips. Finally, he would transfer sperm into the uterus of his mate [2,18–21]. However in reality, young virgin hermaphrodites attempt to crawl away from the male during mating, and depending on the age of the hermaphrodites, their vulval slits can be too tight for males to breach immediately. Thus, the male adopts an alternative behavior, which is to produce high frequency (7–11 Hz) repetitive spicule thrusts at the vulva while maintaining contact with it, until partial spicule insertion induces the full penetration [22–24].

Essential cellular components for spicule insertion were identified in previous work using aged paralyzed hermaphrodites as mates. The movements of the spicules are caused by contractions of the spicule "protractor" muscles, which are attached to the base of the spicules. Rhythmic contractions of

Author Summary

Animal behaviors are generated when a sequence of muscle movements is coordinated by neural circuits. In complex invertebrates or lab-studied vertebrates, due to the large number of cells in their nervous systems and the complexities of their behaviors, it is difficult to address how circuits process information to direct each step of behavior. Here, we used *C. elegans* male mating behavior as a model to address how a compact circuit coordinates different behavioral programs. Male copulation is a multi-step innate behavior, where the male senses his mate, searches for her vulva, then maintains contact with it as he repetitively attempts to insert his copulatory spicules. We demonstrate that the cloacal neurons sense the vulval signal, then command the posterior muscles to contract, so that the male tail sustains contact with the vulva. Simultaneously, via low-resistance electrical connections, the activities of the posterior muscles are relayed to the spicule muscles to cause repetitive spicule insertion attempts. This allows two different behavior patterns to be coordinated. Rhythmic spicule insertion attempts cease and full spicule penetration is induced when multiple contingencies are detected by distinct circuit components.

the protractors, initiated by the postcloacal sensilla neurons PCA, PCB and PCC, cause the spicules to thrust repeatedly against the vulval slit. Tonic contraction of the protractors causes the spicules to extend fully from the male tail and to penetrate the vulva. This step requires the activity of the cholinergic SPC neurons, which innervate the protractors [2,22,25]. Although copulation is initiated by the postcloacal and SPC sensory-motor neurons, it remains elusive how these cells generate and coordinate each step of the behavior.

Understanding the functional cellular/molecular architecture that drives circuit output is a necessity before one can appreciate why certain genes are or are not the evolutionary targets that underlie the diversity of sexual behavior and reproduction. In this study, we addressed how the *C. elegans* male spicule protraction circuit generates and coordinates different motor outputs to penetrate the hermaphrodite's vulva. We determined that stimulation of distinct acetylcholine receptors in posterior sex muscles is used to maintain the male's position over the vulva. This information is simultaneously relayed to the spicule protractors through electrical junctions, thus providing a mechanism for coupling spicule insertion and vulva location behavior. In addition, we identified multiple sensory inputs that control when the protractors should transit from rhythmic to sustained contraction.

Results

Males require cholinergic signaling to maintain contact with the hermaphrodite's vulva during mating

During their attempts to inseminate the hermaphrodite, *C. elegans* males must maintain precise contact between their cloacal opening and the vulva. In our previous study, we observed that males lacking the muscarinic acetylcholine receptor (mAChR) GAR-3 do not sustain their position over the vulva during prolonged attempts to insert their spicules. This mAChR is expressed in the cholinergic spicule-related neurons, PCB and SPC, to enhance ACh secretion from these neurons [26]. ACh secreted from the SPC neurons activates ionotropic ACh receptors on the spicule protractor muscles to induce muscle contraction, which results in tonic spicule protraction [22]. We speculated that

the ionotropic ACh receptors in the cells of the spicule circuit can also be used to sustain precise vulval contact behavior; therefore in the *gar-3* deletion mutant, reduced cholinergic synaptic transmission between the spicule-related neurons and the sex muscles resulted in defective vulval contact.

To address whether ionotropic ACh receptors are utilized to regulate precise vulval contact, we first asked how effectively males that lack the functional levamisole (LEV)-sensitive receptor (L-AChR) mated. The L-AChR had been the only ionotropic ACh receptor described to be involved in ACh agonist-induced spicule protraction. This receptor contains three α-subunits: UNC-38, UNC-63 and LEV-8, and two non-α subunits: UNC-29 and LEV-1 [22,27–30]. We used mutants carrying the *unc-29(e193)* allele, which has a missense mutation that changes a proline to serine at amino acid 258 within the hypothetic first transmembrane domain of the channel [31–33]. LEV induces spicule protraction via activating functional UNC-29-containing L-AChRs, and the effective concentration that induces prolonged protraction for 90% of the males is 2 µM [22]. *unc-29(e193)* males were resistant to LEV. We observed that none of the mutant males protracted their spicules in 2 µM LEV (n = 47), compared to 87.7% of the wild-type males (n = 57, $p < 0.0001$). Like other *unc-29* loss-of-function *(lf)* alleles, the *e193* allele causes worms to have severe uncoordinated locomotion [29,32], which disrupts the males' ability to move backwards along the hermaphrodite during mating. We restored locomotion to the mutant males by using the upstream region of the *acr-8* gene to drive *unc-29* cDNA expression (P*acr-8:unc-29*cDNA::SL2::*GFP*) in the body wall muscles, but not in the male sex muscles [34]. Similar to the *unc-29(lf)* mutant males, the transgenic males were also resistant to LEV; 6% of them protracted their spicules in 2 µM LEV (n = 35, $p = 0.18$). We assayed the mating potency of the locomotion-restored *unc-29(lf)* males by pairing each male with a moving hermaphrodite for 4 hours, and observed that these males could sire progeny with 83.3% of wild-type efficiency (n = 38, Figure 1A). This indicates that even though the L-AChR is used to facilitate spicule protraction in response to LEV, there are other receptors compensating for its function during male mating.

Next, we asked which other ionotropic ACh receptors could be functioning redundantly with the L-AChR. One possibility was the homomeric receptor formed by the α7-like nicotinic ACh receptor (nAChR) subunit, ACR-16. Since it was previously shown to have an ancillary function with the L-AChR in the *C. elegans* locomotion circuit [30,35], we asked if ACR-16 was also used during male mating behavior. After 4 hours of contact with hermaphrodites, males that contained the *acr-16(ok789)* deletion (*acr-16(0)*) achieved 88% of wild-type mating potency (n = 41, Figure 1A), suggesting that like the L-AChR, ACR-16 is not essential for male potency.

We reasoned that if the L-AChR and the ACR-16-containing nAChR were required for mating but were interchangeable, then a severe mating defect would be seen in the *unc-29(lf);acr-16(0)* double mutant. The *unc-29(lf);acr-16(0)* males are completely paralyzed. Since the *acr-16(0)* allele alone does not cause any gross locomotion defect [30,35], we only needed to restore the impaired locomotion of the double mutant using the construct P*acr-8:unc-29*cDNA::SL2::*GFP*. We quantified the velocity of backward locomotion during vulva search behavior and found that the transgenic double mutant males moved relatively well, albeit slightly slower than wild-type males; 105±33 µm/sec for wild type (n = 5 males) and 71±35 µm/sec for the double mutant (n = 5 males) (Figure S1). In our mating potency assay, we found that the transgenic *unc-29(lf);acr-16(0)* males could only achieve 15% of wild-type mating potency (n = 33, $p < 0.001$, Figure 1A). This suggests that both L-AChR and the ACR-16 nAChR are used in
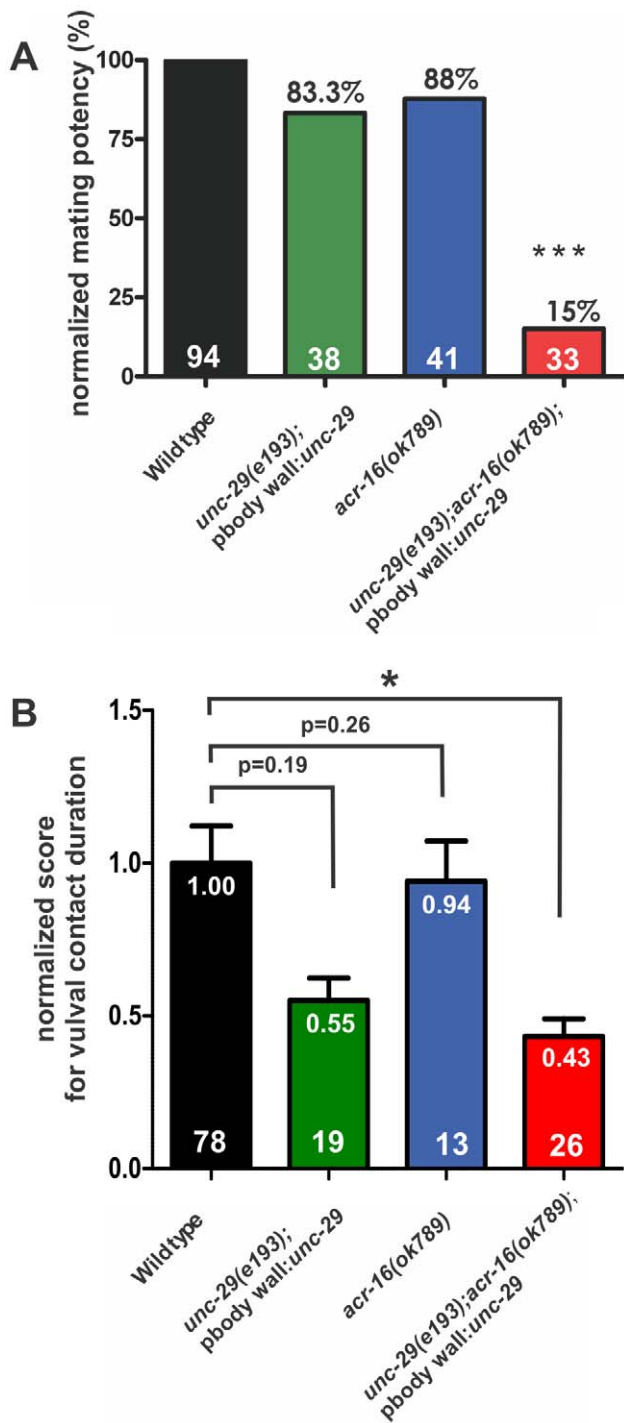
Figure 1. Ionotropic ACh receptors are required for sustained vulval contact. (A) Relative mating potency of mutant males normalized to wild type. The number of males assayed for each strain is listed within each bar. The number above the bar refers to the normalized mating potency value. The males were mated with free-moving hermaphrodites. Each mutant strain was compared to the wild-type males that were assayed in parallel, using the Fisher's exact test. Asterisks (***) indicate the p value <0.0001. (B) Profiles of the vulval contact duration. The males were mated into paralyzed hermaphrodites. The average duration of vulval contact for each male was normalized to the wild type mean to obtain the "normalized score for vulval contact duration", as a measurement of the male's ability to maintain precise vulval contact (Materials and Methods). The mean of the normalized score for vulval contact duration for each strain is represented by the height of the bar, and it is also indicated by the number below the top of the bar. Error bars indicate the standard error of the mean. The number of males assayed for each strain is listed within each bar. Each mutant strain was compared to wild-type males using the Mann-Whitney non-parametric test. Asterisk (*) indicates the p value <0.005. The raw values of average duration of vulval contact for each male tested are presented in Figure S2A.
doi:10.1371/journal.pgen.1001326.g001

male mating behavior, and unlike the locomotion behavior, if the function of one receptor is compromised, the other can equally compensate.

We then asked if the locomotion-restored double mutant males mated poorly because they could not insert their spicules, or if they were additionally defective in other steps of mating, such as maintaining contact with the hermaphrodite's vulva. We paired males with paralyzed *unc-64(lf)* hermaphrodites for them to mate, so that duration of each vulval contact could be accurately recorded [26]. During a 5 minute observation window, the majority of the males we assayed made multiple contacts with the hermaphrodites' vulva before they inserted their spicules or until the observation period ended. Then we determined the average duration of the vulval contacts for each male (Figure S2A). In order to score his ability to maintain precise vulval contact, we first normalized wild type to a score of 1 and then we compared the normalized mutant males to the wild type (Materials and Methods) (Figure 1B). We found that the *unc-29(lf);acr-16(0)* males sustained vulval contact for half the time of wild-type males (p<.05, Figure 1B; see Materials and Methods). In contrast to matings with moving hermaphrodites, the reduced vulval contact did not severely affect the mating potency of the mutant males when they mated with paralyzed hermaphrodites. 48.5% of the double mutant males inserted their spicules and transferred sperm into *unc-64(lf)* hermaphrodites during the 5 minute observation period (n = 33), not statistically different from the 69.7% of the wild type (n = 33, p = 0.13). However, failure to sustain their position over the vulva is likely to be the reason why the double mutant males cannot inseminate free-behaving hermaphrodites, as maintaining contact with a moving object is already challenging for wild-type males: only 10% of the wild-type males could inseminate free-moving hermaphrodites within 5 minutes (n = 20). We then asked if the defect in maintaining vulval contact in *unc-29(lf);acr-16(0)* males was caused by the loss of the L-AChR or the ACR-16 nAChR, or both. Loss of function of either receptor did not reduce the vulval contact duration with statistical significance (Figure 1B), suggesting that these genes are used redundantly to maintain vulval contact. However, although the average duration of vulval contact were not statistically significant between wild type and the mutants, the distributions of vulval contact duration were slightly different (p<0.005, F test; Figure S2A) between wild type and the *unc-29(lf)*, as well as between wild type and the *acr-16(0)* mutant, suggesting that these genes on their own subtly affect the behavior.

The *unc-29* and *acr-16* genes are expressed in the male-specific muscles

We hypothesized that in the *unc-29(lf);acr-16(0)* mutant, signaling from circuit components that maintain vulval contact is impaired, resulting in males that cannot sustain their position at the vulva. To address which neurons and muscles were used in the male mating circuit in this step of behavior, we first determined where *unc-29* and *acr-16* were expressed in the male tail. In adult males, a YFP expression construct that contains a 5.3 kb sequence upstream of the *acr-16* start codon (P*acr-16:YFP*) was observed to
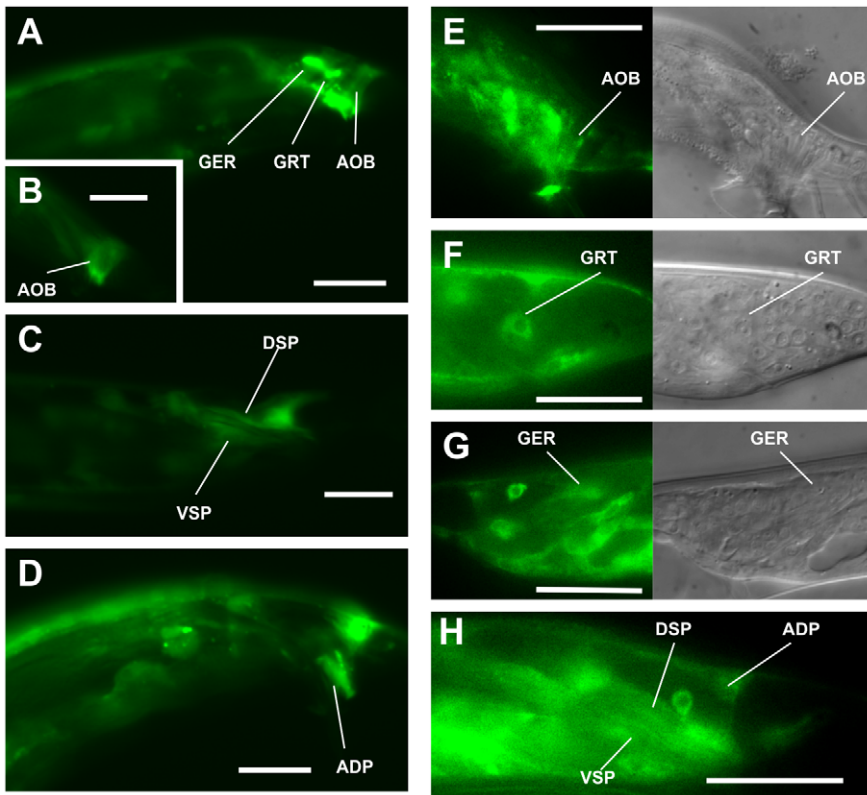
Figure 2. Male tail expression of *acr-16* and *unc-29*. Gubernacular erector (GER), gubernacular retractor (GRT), anterior oblique (AOB), dorsal spicule protractor (DSP), ventral spicule protractor (VSP) and anal depressor (ADP) muscle. (A–D) Fluorescence images of the tail region of adult males expressing the P*acr-16:YFP* construct. Scale bar, 20 μm. (E–H) Fluorescence images of the tail region of adult males expressing the P*unc-29:unc-29::YFP* construct. Scale bar, 20 μm.

be expressed in the body wall muscles, the sexually dimorphic anal depressor muscle, and some male-specific muscles, such as the spicule protractor muscles, the gubernacular erector and retractor muscles and the anterior oblique muscles. However, it was not seen in any neuron in the spicule protraction circuit (Figure 2A-2D). Similarly, a construct that has the 1.3 kb sequence upstream of the first exon of *unc-29* and the whole *unc-29* genomic sequence fused to the YFP gene was expressed in the same set of muscles as well as in some ventral cord neurons and some head neurons. This non-α L-AChR subunit was not expressed on any spicule neuron either (Figure 2E–2H; Figure S3A-S3F).

UNC-63 and UNC-38 are α-subunits required for a functional L-AChR. We found both genes were expressed in the same set of male tail muscles as *unc-29*, but also expressed in the SPC spicule neurons (Figure S3G–S3N). This indicates that UNC-63 and UNC-38 probably form an ionotropic ACh receptor on the SPC neurons independent of UNC-29. UNC-63 and UNC-38 have been found to form a LEV-insensitive ionotropic ACh receptor with the α-subunit ACR-12 and also with the non-α-subunits ACR-2 and ACR-3 on the ventral cord cholinergic motor neurons [36]. This is consistent with the fact that the *acr-12* promoter-genomic DNA fusion construct was also expressed in the SPC neurons (Figure S3O, S3P). Thus, by using the *unc-29(e193)* allele in the *unc-29(e193);acr-16(ok789)* double mutant, we only impaired the function of L-AChR on the male sex muscles. However, it was not initially obvious how reducing UNC-29 and ACR-16 in the sex muscles affected the male's ability to maintain its position over the vulva during spicule insertion attempts.

The postcloacal sensilla neurons maintain the male tail position at the vulva

Electron micrograph reconstruction of the male has reveal extensive electrical and chemical communication between the bilateral sets of muscles and neurons in the tail region (Figure 3A) (S.W. Emmons, personal communication; S.W. Emmons, D.H. Hall, M. Xu, Y. Wang and T. Jarrell, Male Wiring Project, Albert Einstein College of Medicine, http://worms.aecom.yu.edu/pages/male_wiring_project.htm). We studied the connections of the male nervous system to determine candidate neurons that make synapses to the *acr-16* and *unc-29* expressing male sex muscles. Among the muscles that express both *acr-16* and *unc-29*, the spicule protractors are innervated by the SPC cholinergic neurons; the anterior oblique muscles (left/right), and the gubernacular erector (L/R) and retractor (L/R) muscles are innervated by the postcloacal sensilla (p.c.s.) neurons (Figure 3B).

Previous work suggested that the precise location of the vulva is determined by three pairs of p.c.s. neurons, PCA, PCB and PCC. Operated males that contain any two of the three pairs of p.c.s. neurons can sense the precise position of the vulva [2]. However, males with zero or one pair of the p.c.s. neurons can sense the general area of the vulva via the hook sensillum neurons, but will pass over the precise location of the vulva without stopping [2,18]. Although these neurons had been shown to sense the vulva, it had not been determined if they also function in prolonging contact with the hermaphrodite's genitalia.

To assess these neurons' role in maintaining vulval contact, we laser-ablated each individual pair of p.c.s. neurons and tested the male vulval contact efficiency. Similarly to published reports, we
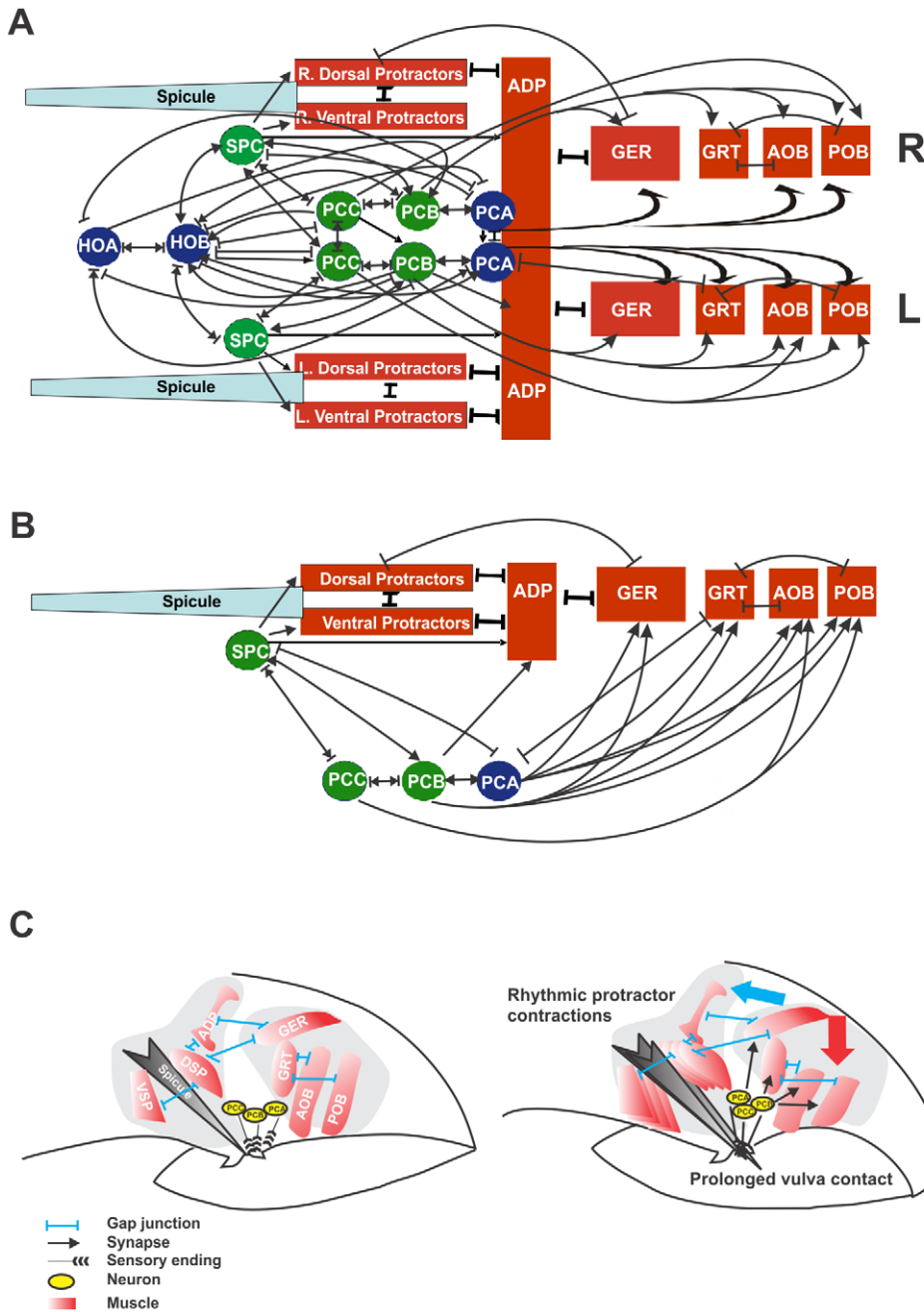
Figure 3. Circuit diagram of cells that control spicule movement and model of prolonged vulval contact coupling to rhythmic protractor contractions. Gubernacular erector (GER), gubernacular retractor (GRT), anterior oblique (AOB), posterior oblique (POB), dorsal spicule protractor (DSP), ventral spicule protractor (VSP) and anal depressor (ADP). Arrows and bars indicate chemical synapses and gap junctions, respectively. Bi-directional arrows refer to cells that make reciprocal chemical synapses. Bi-directional arrows embedded in bars refer to cells that make gap junctions in addition to reciprocal chemical synapses. The green circles refer to cholinergic neurons. (A) Bilateral electrical and chemical connectivity diagram of male neurons and muscles that control the movements of the spicules [adapted from [25], and the Male Wiring Project]. (B) Abbreviated cartoon of limited connections between neurons and muscles discussed in this work. Refer to (Male Wiring Project, Albert Einstein College of Medicine, http://worms.aecom.yu.edu/pages/male_wiring_project.htm) for a more complete list of connections to other cells in the male. (C) Cartoon depicting changes in male tail muscles upon vulval contact. Left panel depicts relative locations and electrical junctions between the male sex muscles. The right panel depicts the shortening of the AOB and POB muscles causing a curvature in the posterior male tail (red arrow) upon chemical stimulation from the PCA, PCB and PCC neurons. Stimulated GER muscles relay their signals to the spicule protractor muscles causing rhythmic contractions (blue arrow).
doi:10.1371/journal.pgen.1001326.g003

found that ablations of any neuronal pair do not obviously affect the males' ability to locate the precise position of the vulva, since the other two pairs can compensate (data not shown). However, like the *unc-29(lf);acr-16(0)* males, the operations significantly reduced the duration of vulval contact (Figure 4A; Figure S2B), suggesting that each pair of p.c.s. neurons is used to sustain contact between the cloacal opening and the hermaphrodite's vulva. Among these neurons, the PCB and PCC neurons are cholinergic
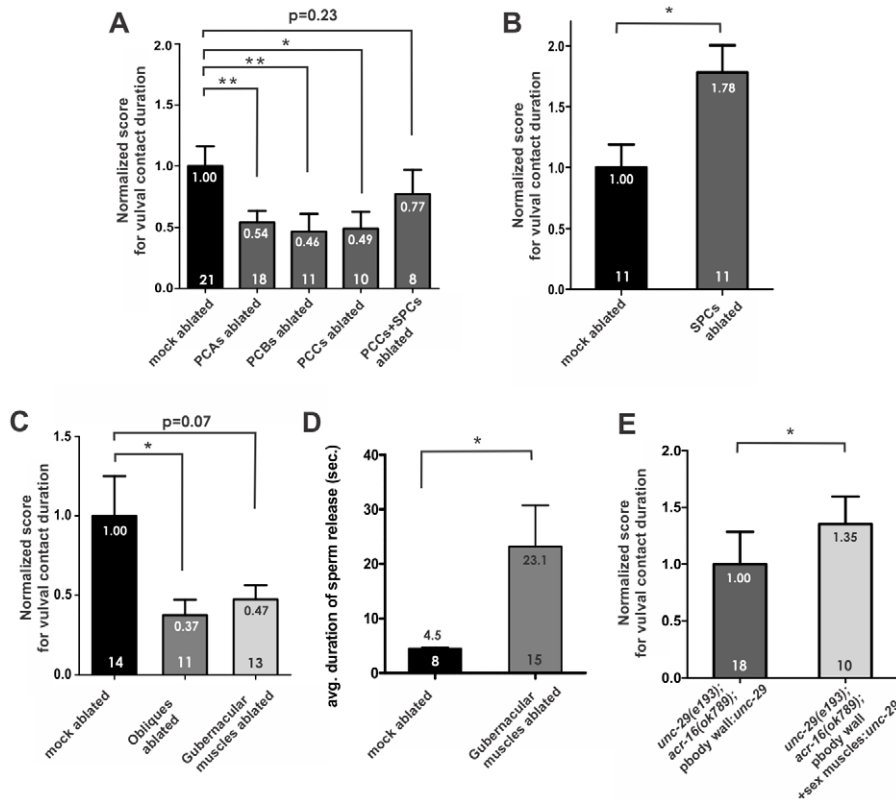
Figure 4. The postcloacal sensilla (p.c.s.) neurons and the oblique muscles facilitate prolonged vulval contact. (A–C) The average duration of vulval contact for each male was normalized to the mock-ablated mean to obtain the "normalized score for vulval contact duration" (Materials and Methods). The mean of normalized score for each strain is represented by the height of the bar, and it is also indicated by the number below the top of the bar. Error bars indicate the standard error of the mean. The number of males assayed for each operation is listed within each bar. Ablated males are compared to mock-ablated males that mated with the same group of hermaphrodites. Data that are shown in the same panel were obtained in parallel, but cannot be compared directly to data presented in different panels. (D) Ablation of the gubernacular muscles increases the duration of sperm release. The average duration of sperm release is represented by the height of the bar, and it is also indicated by the number below the top of the bar. The number of males assayed for each operation is listed within each bar. Error bars indicate the standard error of the mean. (E) Restoring *unc-29* in male muscles reverses the vulval contact defect of the locomotion-restored *unc-29(lf);acr-16(0)* males. The average duration of vulval contact for each male was normalized to the mean of the body wall muscle *unc-29* rescued males, to obtain the "normalized score for vulval contact duration". The mean of normalized score for each strain is represented by the height of the bar, and it is also indicated by the number below the top of the bar. The number of males assayed for each operation is listed within each bar. Error bars indicate the standard error of the mean. Asterisks (**) indicate the *p* value <0.005, (*) indicates the *p* value <0.05, calculated using the Mann-Whitney non-parametric test. The raw values of average duration of vulval contact or duration of sperm release for each male tested are presented in Figure S2B-S2F.
doi:10.1371/journal.pgen.1001326.g004

[22]. The non-cholinergic PCA neurons might exercise this function using other neurotransmitters.

The cholinergic SPC neurons innervate the spicule protractor muscles and are required for sustained protractor contraction, which results in keeping the spicules inserted into the hermaphrodite's vulva during sperm transfer [22,25]. We observed the effect of ablating the SPC neurons on vulval contact duration, and found that unlike the p.c.s. operations, the SPC-ablated males could stay at the vulva of paralyzed hermaphrodites significantly longer than the intact control males (Figure 4B; Figure S2C). This increase in duration is not a simple result of the failure to insert the spicules, since hermaphrodites used for this assay were purposely chosen to be difficult for intact males to penetrate. Additionally, intact control males that were observed to penetrate the hermaphrodite, inserted their spicules after multiple vulval contacts, and multiple contacts were recorded for the SPC operated males as well (see Material and methods). In addition, ablating the SPC neurons could reverse the vulval contact deficiency caused by ablation of an individual pair of p.c.s. neurons (PCCs) (Figure 4A; Figure S2B). These indicate that,

unlike the p.c.s. neurons, the SPC neurons are not required to sustain contact with the vulva, but might be involved in delimiting the duration of this step in mating behavior.

The oblique muscles are required for prolonging vulval contact

To test the hypothesis that the male p.c.s. neurons maintain vulval contact by innervating the *acr-16* and *unc-29* expressing sex muscles, we ablated the oblique muscles and the gubernacular muscles, to see which operation causes defects similarly to the p.c.s. ablations. We ablated both anterior and posterior oblique muscle nuclei in L4 males. The anterior and posterior oblique muscles lie dorsal-ventrally at the male tail near the cloacal opening, having both the dorsal and ventral ends attached to the body wall [25,37]. Similarly to intact males, the operated males initiated backward scanning of the hermaphrodites, and they paused at the vulva and started to prod the vulva with their spicules. However, they lose vulval contact and resumed backward scanning more frequently than non-ablated males (Figure 4C, Figure S2D). The vulval contact that remained was largely due to

the hermaphrodites being paralyzed. When paired with free-moving hermaphrodites, the males could not maintain the contact (average duration = 2 seconds, n = 3). The contraction of the oblique muscles might change the tail posture during mating, based on their position and shape in the male tail. We propose that contractions of these muscles sustain vulval contact through the application of force between the male cloaca and the hermaphrodite's vulva.

We then laser ablated the gubernacular erector and retractor muscles on both sides of the males at the early L4 larval stage, and observed their mating behavior when they became adults. The gubernaculum is a cuticle structure that lies posterior to the spicules, and it is thought to help guide the extension of the spicules through the male cloaca. The gubernacular erectors and retractors are muscles that attach the gubernaculum to the body wall [25,37]. We found that the vulval contact duration for these males was slightly, but not significantly shorter than the wild type (Figure 4C; Figure S2D); suggesting that unlike the oblique muscles, the gubernacular muscles are not essential to sustain vulval contact.

Strikingly, the gubernacular muscle-ablated males showed difficulty in sperm transfer (Figure 4D; Figure S2E). In intact males, after sperm leaves the seminal vesicle, the gametes are briefly held at the distal end of the vas deferens for two to four seconds, until they are "released" out of the cloaca [2,20]. In gubernacular muscle-ablated animals, sperm accumulated at the distal end of the vas deferens and did not efficiently drain out of the male. In contrast, from casual observation, ablating oblique muscles or other spicule-associated neurons described in this work did not seem to affect this step of behavior. Sperm transfer requires signals from ventral cord neurons, the gonad and the SPV spicule sensory neurons [2,20,38]. We speculate that the gubernacular muscle contractions move the gubernaculum, which lifts the adjacent tissues so that the lumen of the distal vas deferens is accessible to the cloacal opening.

The LEV-sensitive ACh receptor functions in the male sex muscles to facilitate vulval contact

Previous data suggest that the p.c.s. neurons facilitate the males' contact with the vulva through stimulating ionotropic ACh receptors on the postsynaptic oblique muscles. However, given the expression pattern of unc-29, it is also possible that the behavior is regulated by the L-AChRs on the ventral cord or head neurons. Therefore, we asked if restoring the L-AChR in the male sex muscles could reverse the vulval contact defect in the unc-29(lf);acr-16(0) males. We restored unc-29 cDNA in the body wall muscles and the male sex muscles using the 3.5 kb promoter region of the tropomyosin gene lev-11 [6] (Plev-11:unc-29cDNA::SL2::GFP). Compared to unc-29(lf);acr-16(0) males that had unc-29 expressed only in the body wall muscles, males that expressed unc-29 in both body wall and sex muscles could sustain vulval contact significantly longer (Figure 4E; Figure S2F), suggesting that the L-AChR functions in the male sex muscles to facilitate vulval contact.

The gubernacular-oblique muscle group activity directly induces repetitive protractor muscle contractions

At the vulva, the male coordinates movements of multiple muscles in his tail to effectively penetrate the vulval slit. While he maintains his precise position at the vulva via the oblique muscles, his spicules are rapidly prodding the vulval slit as a result of repetitive protractor muscle contractions. The postcloacal sensilla initiate the spicule prodding behavior [22]; however, the postcloacal sensilla neurons do not make synapses to the protractor muscles (Figure 3B; Male Wiring Project).

The gubernacular erectors and retractors, as well as the anterior and posterior oblique muscles, are innervated by two of the three pairs of p.c.s. neurons or all three of them (Figure 3B), and it is likely that these muscles are stimulated simultaneously when the p.c.s. neurons become activated. In addition, the gubernacular retractors make gap junctions to both the anterior and the posterior oblique muscles (Male Wiring Project; Figure 3B). We therefore refer to these muscles as the "gubernacular-oblique muscle group". Interestingly, the spicule protractor muscles and the anal depressor muscle are also connected to the gubernacular erectors through gap junctions (Male Wiring Project; Figure 3B). Since gap junctions are low-resistance channels that bridge two cells and allow ions to pass directly, the cytoplasm of the cells are connected, and cell activity can be synchronized by exchanging electric transients [39,40]. We then hypothesized that ions or other signal molecules could pass from the gubernacular-oblique muscle group through the gap junctions to induce Ca^{2+} transients in the protractor and the anal depressor muscles. In this way, by innervating the gubernacular-oblique muscle group, the p.c.s. neurons could initiate repetitive contractions of the protractors.

To test our hypothesis, we asked if localized activation of the gubernacular-oblique muscle group could immediately induce fast repetitive protractor muscle contractions and Ca^{2+} transients in these muscles. We employed the YFP-fused channelrhodopsin-2 light-gated cation channel (ChR2::YFP) to depolarize the gubernacular-oblique muscle group [41]. The 6.2 kb region upstream of the acr-18 gene was used as the promoter to drive transcription of ChR2::YFP in multiple cells, including the gubernacular erector and retractor muscles and the posterior oblique muscles, but not the spicule protractors (Figure S3Q and S3R). When ChR2 was expressed and activated by growing males in the presence of all-trans retinal, the activating blue light caused the spicule protractors to contract repetitively. When multiple sequential brief pulses of blue light were applied, the repetitive spicule movements were induced correspondingly, and coupled to the light stimulation (Figure 5A; Figure S4; Figure S5A-S5C; Video S1; see Materials and Methods). In contrast, males that grew in the absence of all-trans retinal did not respond to light stimulation (Figure 5A; Figure S5D-S5E; Video S2), since the blue light-induced transients require the presence of all-trans retinal [42].

To verify that the repetitive spicule movements were directly due to protractor muscle contractions and not to non-specific displacement of neighboring tissue, we measured Ca^{2+} dynamics in the spicule muscles. To detect Ca^{2+} level changes in the protractor muscles and the anal depressor muscle, we expressed a fluorescent Ca^{2+} indicator protein, G-CaMP, using one of the unc-103 promoter regions (Punc-103E) [5,43,44], and expressed a red fluorescent protein (DsRed) using the same promoter as an internal control (Pacr-18:ChR2::YFP+Punc-103E:G-CaMP+Punc-103E:DsRed) [5,45,46]. Ca^{2+} transients were determined by changes in the G-CaMP/DsRed intensity ratio in the same tissue. The excitation spectrum of G-CaMP overlaps with ChR2 [43,47]. To determine the baseline of the G-CaMP/DsRed intensity ratio in the protractor-anal depressor muscles (in the absence of ChR2-mediated gubernacular-oblique muscle activation), males were first imaged under the blue excitation light prior to exposure to all-trans retinal. Afterwards, they were incubated on plates that contained all-trans retinal for 30 minutes and then reimaged again under the blue light. 30 minutes of incubation was sufficient to activate ChR2 for light stimulation (Figure S6). In the presence of all-trans retinal, we observed Ca^{2+} transients in correlation with light-induced contractions that caused muscle length changes (Figure 5B, 5C; Video S3; see Materials and Methods). In
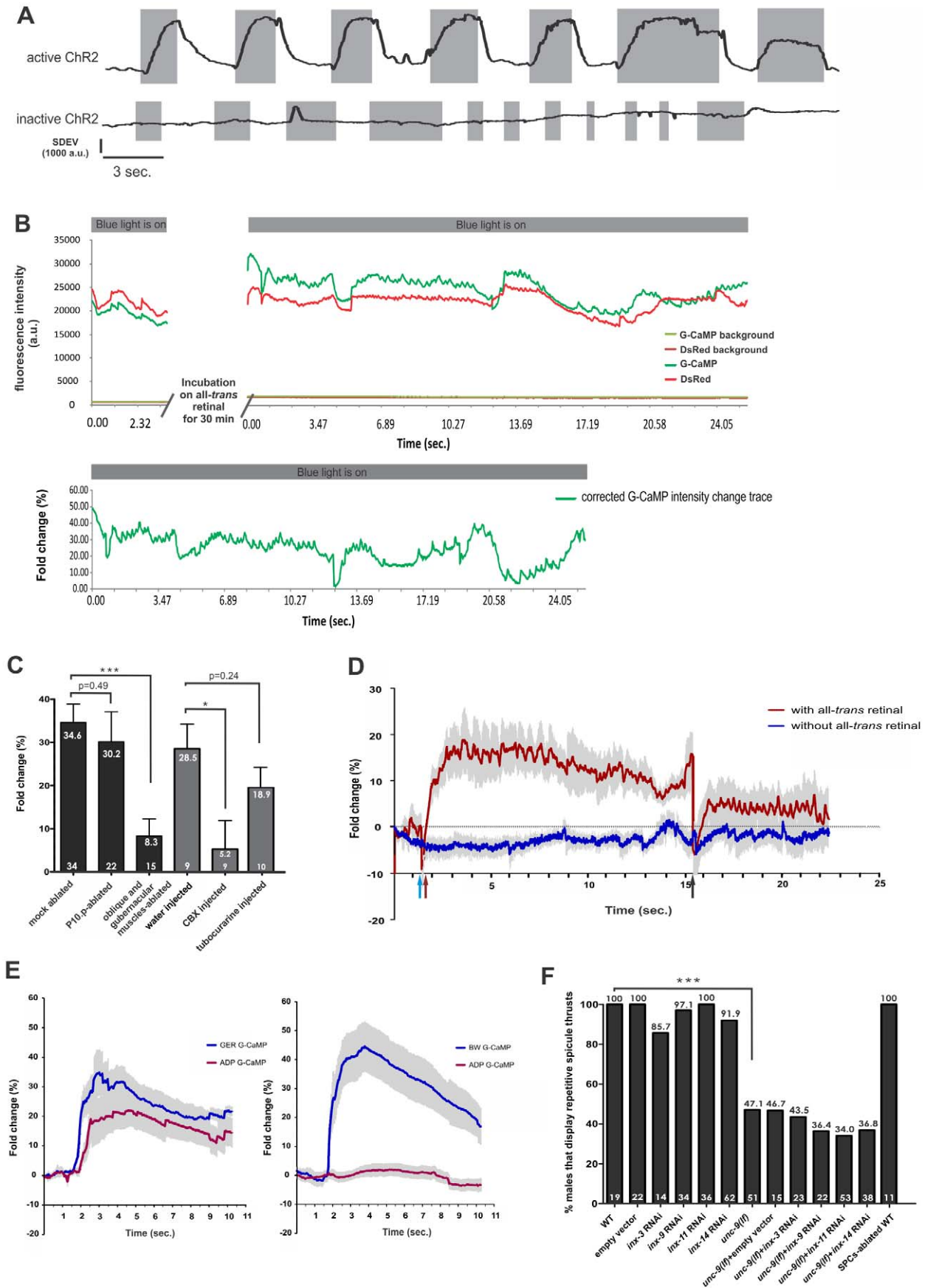
Figure 5. Stimulation of the gubernacular-oblique muscle group induces repetitive spicule thrusts and Ca²⁺ transients in the spicule protractor-anal depressor muscles. (A) Displacement of the spicule during and between brief blue light pulses. The grey regions indicate the time periods of blue light pulses. An image sequence of the male tail was captured for ~30 seconds when light pulses were applied repetitively. A region of interest (ROI) was placed at the base of a spicule, and the standard deviation of the pixel intensity within the ROI was obtained to indicate spicule displacement (see Materials and Methods). A representative trace for males that expressed active ChR2 (in the presence of all-*trans* retinal) is shown in the upper panel; a representative trace for males that expressed inactive ChR2 (in the absence of all-*trans* retinal) is shown in the lower panel. a.u. arbitrary units. (B) Raw fluorescence and corrected intensity traces for a representative male. Upper panel: raw fluorescence intensity traces in the protractor without gubernacular-oblique muscle stimulation for the baseline recording (with inactive ChR2), and during stimulation of active ChR2 on the gubernacular-oblique muscle group. Fluorescence intensity for both G-CaMP and DsRed channels are plotted, as well as the background fluorescence intensity for each channel. The periods that the light stimuli were applied are indicated by grey bars; the numbers on the X-axis indicate the time points since the onset of the most recent light stimulus; the 30 minute incubation is indicated on the X-axis. a.u. arbitrary units. Lower panel: corrected G-CaMP fold change trace during light stimulation with active ChR2. (C) Maximal G-CaMP intensity changes in the protractors during light stimulation. The number of males assayed for each operation is listed at the bottom of each bar. The numbers below the top of the bars indicate the mean of maximal G-CaMP intensity changes of the population. Error bars indicate the standard error of the mean. Asterisk (***) indicate the p value <0.0005, (*) indicates the p value <0.05, calculated using the Mann-Whitney non-parametric test. (D) Average G-CaMP intensity changes before, during and after a pulse of blue light stimulation. The blue arrow indicates the beginning of light stimulation, the red arrow indicates the onset of G-CaMP intensity increase, and the black arrow indicates the end of light stimulation. The trace in red represents males with active ChR2. Males without active ChR2 are represented by the blue trace. The grey region around each curve represents the standard error of the mean. 4 males were measured for each trace. (E) Averaged G-CaMP intensity change traces in the anal depressor muscle (ADP), the gubernacular erector (GER) and a posterior body wall muscle (BW), upon laser microbeam stimulation of the gubernacular erector muscle or the posterior body wall muscle in the male tail. Traces represent averaged G-CaMP intensity changes in specific muscles. The grey region around each trace represents the standard error of the mean. Left panel, the gubernacular erector on one side of the males was stimulated by a laser microbeam. The energy of the laser was adjusted to the lowest level that could elicit Ca²⁺ transients in the muscles. N = 10 males. Right panel, a body wall muscle that has no gap junction to the protractor-anal depressor muscle group was stimulated by a laser microbeam. Ca²⁺ transients in the gubernacular erector and the anal depressor muscles were detected by using G-CaMP. Stimulation of the posterior body wall muscle failed to induce Ca²⁺ transients in the anal depressor muscle, indicating that in the left panel, Ca²⁺ transients in the anal depressor muscle were not caused by non-specific laser damage in the male tail. N = 11 males. (F) Effects of innexin mutant, RNAi of innexins and SPC ablation on ChR2-induced spicule thrusts. The *unc-9(lf)* males were compared to the wild type. The innexin RNAi strains with a wild-type genetic background were compared to the wild type that was fed with empty vector. The innexin RNAi strains with an *unc-9(lf)* genetic background were compared to the *unc-9(lf)* that was fed with empty vector-containing bacteria. The SPC-ablated wild type was compared to un-operated wild type. The numbers above the bars show the percentage of males that displayed rapid spicule thrusts upon light stimulation. The number of males assayed for each strain is listed within the bar. Asterisks (***) indicate the p value <0.0001, using the Fisher's exact test.
doi:10.1371/journal.pgen.1001326.g005

contrast, ChR2-expressing males that grew in the absence of all-*trans* retinal, did not display spicule thrusts or had Ca²⁺ transients in the protractor muscles (data not shown, n = 30; Video S4).

P*acr-18:ChR2::YFP* was also expressed in the HOA hook sensillum neuron (Figure S3T-S3V), which theoretically could induce the spicule prodding behavior independent of the p.c.s. neurons [22]. To rule out the possibility that Ca²⁺ transients we observed in the protractor muscles were the result of HOA neuron activity, we laser ablated the hook sensillum precursor cell P10.p in the late L2 larval stage (see Materials and Methods). When we activated ChR2 in the gubernacular-oblique muscle group of ablated adult males, we found that Ca²⁺ transients in the protractor muscles were still induced with a magnitude that was slightly, but not significantly lower than mock-ablated males (p>0.05, Figure 5C). This result suggests that under these conditions, HOA is not the major contributor for Ca²⁺ transients observed in the spicule protractor muscles.

To verify that Ca²⁺ transients observed in the protractor muscles were caused by excitation of the gubernacular-oblique muscle group, we ablated the gubernacular erector and retractor muscles and the anterior and posterior oblique muscles. We found that the repetitive contractions of the protractors were impaired, and Ca²⁺ transients observed in the ablated animals were greatly reduced (p<0.0005, Figure 5C). We reasoned that ablating nuclei at the mid-L4 larval stage severely impaired the physiology of these muscle cells and reduced the amount of ChR2 proteins on the remaining cell membranes. Thus, the cell corpses that remained after ablation could not be activated sufficiently to pass ions or signal molecules to the protractors to induce detectable Ca²⁺ transients. The remaining activity we saw in the protractors could be due to activity in the sphincter muscle and the spicule retractor muscles, since the upstream region of *acr-18* also drove transcription in these muscles (Figure S3R, S3S). These muscles are also connected to the spicule protractors through gap junctions

(Male Wiring Project). However in an intact male, due to the lack of innervation from male-specific neurons (Male Wiring Project), the sphincter and spicule retractor muscles are not likely to be the major facilitators of rhythmic spicule prodding behavior. These observations suggest that direct depolarization of the gubernacular-oblique muscle group in the absence of neuronal input can elicit Ca²⁺ transients in the protractor-anal depressor muscles to induce muscle contraction.

To gain a better idea of the temporal correlation between gubernacular-oblique muscle group depolarization and protractor-anal depressor muscle activities, we monitored Ca²⁺ levels continuously in the protractor muscles before, during and after a brief pulse of blue light stimulation of the gubernacular-oblique muscles. Using a Mosaic Imaging System (Andor™ Technology), we excited multiple regions simultaneously or sequentially without optically stimulating the whole field of view. We found that Ca²⁺ levels elevated gradually in the protractor muscles upon light-activation of the gubernacular-oblique muscles, and declined rapidly after the stimulation (Figure 5D; Video S5, S6; see Materials and Methods). We also stimulated the gubernacular erector muscles using a laser-induced muscle contraction method [48]. In males that did not express ChR2, abrupt release of internal Ca²⁺ stores in the gubernacular erector muscle, via irradiating the muscle with a low-energy laser microbeam (440 nm), also elicited Ca²⁺ transients in the protractor-anal depressor muscles, causing rapid muscle contraction (Figure 5E; Video S7, S8; see Materials and Methods). Interestingly, in both the optical and the laser stimulation of the gubernacular muscles, Ca²⁺ transients in the protractor and anal depressor muscles are induced with a delay of up to 0.3 seconds (Figure 5D; Figure 5E). The similar latency was also observed for light-induced spicule thrusts (Figure 5A; Figure S5). We speculate that this period is required for Ca²⁺ to travel between the muscles through gap junctions. Similar phenomenon was also observed in the *C. elegans*

intestinal cells. Adjacent cells that are connected by gap junctions showed Ca^{2+} spikes that were not complete synchronous [49]. We therefore suggest that activities of the gubernacular-oblique muscle group, initiated by the p.c.s. neurons, can be transmitted to the spicule protractor muscles directly, probably through gap junctions.

Gap junctions are required for information transmission from the gubernacular-oblique muscle group to the protractor muscles

To determine if gap junctions mediate the activity transmission between the gubernacular-oblique muscles and the protractor-anal depressor muscles, we asked if the application of a gap junction inhibitor could affect Ca^{2+} transients in the protractor-anal depressor muscles during gubernacular-oblique muscles stimulation. Carbenoxolone (CBX) has been shown to inhibit innexin function in invertebrates [50-52]. We found that application of this drug reduced the light-induced Ca^{2+} transients in the protractor-anal depressor muscles (Figure 5C; Figure S7). To the contrary, application of tubocurarine, which blocks both nicotine-sensitive and LEV-sensitive AChRs, [27,29,30,53,54] and cause the males to be paralyzed, did not affect either repetitive protractor contractions or Ca^{2+} transients in response to light stimulation (Figure 5C). Although it is possible that ChR2-stimulation of the gubernacular-oblique muscles could indirectly cause some non-specific neuron to secrete neurotransmitters other than ACh to induce Ca^{2+} transients in the spicule protractor-anal depressor muscles, the tubocurarine result in conjunction with the CBX experiment indicates that functional gap junctions, instead of cholinergic synaptic transmission, are required for activities of the gubernacular-oblique muscles to be relayed to the spicule protractor muscles.

The *C. elegans* genome encodes 25 innexin proteins. To identify the innexin(s) that is important to the coupling of male sex muscles, we first determined innexin genes that are expressed in these muscles. A high-resolution expression map of all innexins has been reported in the *C. elegans* hermaphrodite, and five innexins are expressed in the hermaphrodite sex muscles: *inx-3*, *inx-8*, *inx-9 inx-14* and *unc-9* [55]. In addition, *inx-11* was reported to be expressed in these muscles as well in another study [56]. The hermaphrodite sex muscles are derived from the M-lineage, same as the male sex muscles [57]; hence, it is possible that these genes are also expressed in the male sex muscles. We inspected these genes' expression patterns in males by checking GFP expression under the control of their promoter regions [55]. We found that *unc-9* and *inx-14* are expressed in multiple male-specific sex muscles and the sexually dimorphic anal depressor muscle. In addition, *unc-9* is also expressed in the SPC and the PCB neurons in the male tail (Figure S8).

To test if these innexins are used to transmit signals among the male sex muscles, we asked if the light-induced rapid thrusts of the spicules are affected when these genes are mutated or knocked-down by RNA interference (RNAi). Males that carry the *unc-9(e101)* loss-of-function allele have uncoordinated locomotion [58], probably due to inhibited electrical coupling among body wall muscles, as well as neuronal UNC-9 deficiency [59]. We found that when ChR2 was expressed in the gubernacular-oblique muscles in these males, in the presence of all-*trans* retinal, only 47.1% of the males responded to the blue light with repetitive spicule thrusts (n = 51, p<0.0001), compared to 100% of the wild type (n = 19; Figure 5F). To the contrary, light-induced spicule thrusts were not affected by RNAi of *inx-3*, *inx-9*, *inx-11* or *inx-14*. In addition, RNAi of these genes in the *unc-9(e101)* genetic background did not result in further inhibition of the behavior (Figure 5F). In theory, the reduced spicule thrusts can be resulted

from a deficiency of UNC-9 in the SPC and PCB neurons. We addressed this possibility by first asking if these neurons are required for blue light-induced spicule thrusts. We reasoned that the PCB neurons do not make synapse or gap junction to the protractors; as a result, for the PCBs to mediate the "muscle-induced muscle contraction" phenomenon, they have to send signals through the SPC neurons, which innervate the protractors. Therefore, we can test whether the PCB and SPC neurons are required for the "muscle-induced muscle contraction" phenomenon by asking if light-stimulated gubernacular-oblique muscle activity can still induce spicule thrusts when the SPC neurons are ablated. We found that ablation of the SPC neurons did not have an effect (Figure 5F), suggesting that neither pair of these neurons is required and therefore a deficiency of UNC-9 in these neurons is not likely to cause reduced light-induced spicule thrusts. Taken together, these data suggest that the UNC-9 innexin is used in some of the gap junctions that mediate the direct signal transmission from the gubernacular-oblique muscles to the protractor-anal depressor muscles. Identification of additional gap junction subunits awaits further study.

The SPC neurons are necessary, but not sufficient to trigger sustained protractor contraction

Repetitive protractor contractions eventually transform into a tonic contraction, which causes the spicules to penetrate the vulva. Premature tonic protractor contraction, prior to or during the various sub-steps of mating, rarely occurs in wild-type males [60], suggesting that the triggering of tonic protractor contraction is under strict regulation. We favored the hypothesis that multiple signals are integrated by the spicule circuit to induce sustained protractor contraction at the proper moment of mating.

We used ChR2 to activate subsets of spicule circuit components, in males that were not engaged in mating [41,61-63], and then asked if these cells could induce sustained spicule protraction (Figure 6A). To our surprise, when we expressed ChR2 in all muscles, using the tropomyosin P*lev-11* promoter (P*lev-11:ChR2::YFP*), we observed that blue light induced strong body wall muscle contraction in all males, but only 5% of them displayed tonic contraction of the protractors. The remaining males responded to blue light with shallow repetitive protractor contractions with the tips of their spicules slightly protruding from the cloacal opening (n = 20, Figure 6B, Video S9). Consistent with this result, expressing ChR2 in sex muscles (the spicule protractors, the gubernacular erector and retractor muscles, the anterior and posterior oblique muscles, the sphincter and the diagonal muscles) and the sexually dimorphic anal depressor muscle, using the P*unc-103E* promoter (P*unc-103E:ChR2::YFP*), also induced repetitive shallow protractor contractions. Approximately 18% of males fully protracted their spicules (n = 17, Figure 6B, Video S10). Since light-activated ChR2 channels should depolarize the muscle cells, we speculated that some negative regulatory molecules on the spicule muscles might be keeping them from contracting tonically.

To address if spicule activity is controlled by negative regulator molecules, we introduced a null allele of the *unc-103* gene (*n1213*) into the P*unc-103E:ChR2::YFP*-expressing animals. The *unc-103* gene encodes an ERG-like K^+ channel. The *unc-103* deletion males (*unc-103(0)*) occasionally protract their spicules in the absence of mating stimulation. Previous studies suggested that the K^+ channel suppresses premature spicule protraction by reducing the excitability of the spicule muscles [44,60]. In *unc-103(0)* males that expressed ChR2 on their sex muscles, blue light induced tonic spicule protraction in 93.8% of the population (n = 16, Figure 6B; see Materials and Methods). In contrast, the transgenic male population that grew in the absence of all-*trans*
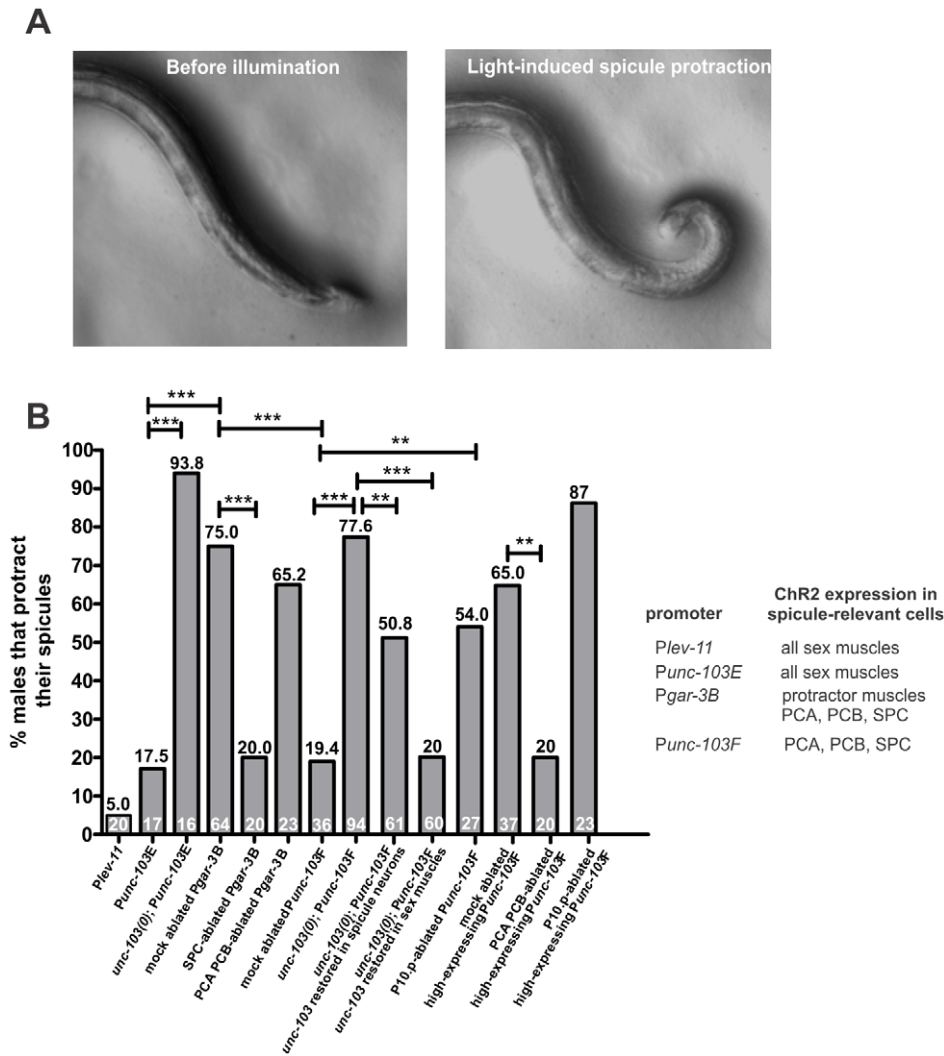
Figure 6. Stimulation of ChR2 in different spicule circuit components. (A) Left panel, a male that expresses P*gar-3:ChR2::YFP* holds his spicules inside of his tail prior to illumination. Right panel, the blue light induces sustained spicule protraction of this male. (B) Sustained spicule protraction induced by stimulation of ChR2 in different circuit components. The numbers on the vertical axis represent the percentage of males that protracted their spicules when different circuit components were activated by light-stimulated ChR2. The numbers above the bars show the percentage of males that protracted their spicules. The number of males assayed for each strain is listed within the bar. Asterisks (***) indicate the p value <0.0001, (**) indicate the p value <0.001, using the Fisher's exact test.
doi:10.1371/journal.pgen.1001326.g006

retinal did not protract their spicules under the blue light (n = 20). This suggests that in wild-type males, the UNC-103 K$^+$ channel functions on the spicule muscles to counteract the ChR2-mediated depolarization.

The transition between protractor contractile states is presumed to be facilitated by the cholinergic SPC neurons. These neurons have proprioceptive sensory endings that are attached to the protractor muscles and are suggested to sense the spicule position in the vulval channel. Removal of these cells results in operated males that rhythmically prod the vulva with their spicules, but never completely insert them during mating [2,22]. Since these neurons make synapses to the muscles, their secretions might be sufficient to evoke tonic muscle contraction. Alternatively, the ACh signals from the SPC neurons might need to act in conjunction with the rhythmically contracting protractors to induce the state change in the muscles.

To test these hypotheses, we used the promoter region of the *gar-3* gene (P*gar-3B:ChR2::YFP*) to express ChR2 in the SPC neurons and two of the p.c.s. neurons (PCA and PCB), in addition to the spicule protractors and the anal depressor [26]. 75% of the males responded to the fluorescent light with sustained spicule protraction (n = 64, Figure 6A and 6B; Video S11). To verify that this was due to SPC neuron activity, we laser ablated these cells, and found that blue light only caused sustained protraction in 20% of the males (n = 20, Figure 6B). In addition, ablation of the PCA and PCB neurons did not affect the light-induced behavior (n = 23, Figure 6B), presumably since the spicule muscles were already stimulated via P*gar-3B*-expressing ChR2 and did not require further p.c.s. signaling.

If the p.c.s. neurons induce rhythmic spicule protractor contractions, and activation of the SPC neurons switches rhythmic contractions to tonic contraction, then artificially activating these neurons independent of the spicule muscles should cause sustained spicule protraction. To test this, we used one of the *unc-103* gene promoter regions (P*unc-103F*) to express ChR2 in the PCA, PCB and SPC neurons [44]. Only 19.4% of males, the ones that highly

expressed P*unc-103F:ChR2::YFP*, displayed prolonged protractor contraction in response to blue light (n = 36, Figure 6B). When we preselected males that displayed very high expression of P*unc-103F:ChR2::YFP*, 65% of these biased males displayed the behavior after light stimulation (n = 37, Figure 6B). Laser ablation of the PCA and PCB sensory neurons reduced the percentage of light-stimulated protraction in preselected biased males to 20% (n = 20, *p* = 0.002), indicating that stimulation of the SPC neurons in the absence of PCA and PCB activity does not result in efficient tonic muscle contraction.

The low efficiency of P*unc-103F:ChR2::YFP*-induced spicule protraction in unbiased males suggested that the spicule-prodding/protraction neurons have intrinsic properties, which to overcome, require high levels of ChR2 stimulation. We reasoned that, similar to the spicule muscles, the UNC-103 K$^+$ channel might be offsetting ChR2 activity in the spicule neurons. When the P*unc-103F:ChR2::YFP* construct was introduced into the *unc-103(0)* males, 77.6% of the population fully protracted their spicules in response to the blue light (n = 94, Figure 6B). The *unc-103* gene is expressed in both spicule-associated neurons and the male sex muscles [6,44]. We found that restoring functional UNC-103 in the sex muscles could reestablish these males' resistance to light-stimulation; however, expressing *unc-103* in the spicule-associated neurons can also restore some resistance to light stimulation (Figure 6B). Thus in wild type, the UNC-103 channel likely regulates the excitability threshold of neurons, in addition to muscles.

Why do the p.c.s. and SPC neurons promote spicule protraction at the vulva, but not efficiently under artificial non-mating conditions? We hypothesized that in addition to UNC-103, the activities of the p.c.s. and SPC neurons might be attenuated by other neurons. In intact males, spicule prodding and full protraction only occur when the males are at the vulva, which is sensed by both the p.c.s. and the hook sensillum. When the hook sensillum precursor cell, P10.p is laser-ablated, the operated males no longer sense the general area of the vulva but instead randomly prod the cuticle of the hermaphrodite with their spicules [2]. This suggests that in intact males, the cells derived from P10.p might attenuate spicule protractor activity at areas outside the vulva. The P10.p precursor cell gives rise to the hook structural cells, HOA and HOB sensory neurons and the PVZ motor neuron. The PVZ does not make synapses to the spicule-relevant neurons, but the HOA and HOB hook sensillum neurons do make direct chemical and electrical connections to the p.c.s. and SPC neurons (Figure 3A; Male Wiring Project). Thus, it is possible that these connections might negatively modulate spicule activity until the vulva is sensed.

We ablated the precursor cell P10.p in P*unc-103F:ChR2::YFP*-expressing males, and found that in 54% of unbiased operated males (n = 27, Figure 6B) and 87% of high-expressing operated males (n = 23, Figure 6B), the light induced prolonged protraction. In both cases, the incidence of ChR2-induced spicule protraction was higher in operated animals compared to mock-ablated. However, for unbiased males, the difference was statistically significant (*p* = 0.004), whereas for biased P*unc-103F:ChR2::YFP* high-expressing males, the increase was not statistically different over the already high protracting non-ablated males (*p* = 0.08). We conclude that the lineage descendants of P10.p, most likely the hook neurons, can reduce the output of ChR2-activated p.c.s. and SPC neurons, but this reduction can be partly circumvented by expressing more ChR2.

Discussion

C. elegans male mating behavior is a multi-step goal-directed behavior that utilizes several active sensing processes, as the male worm actively acquires sensory inputs using different types of "motor sampling routines" [64]. For example, sensation of the hermaphrodite during male locomotion initiates the backward vulval searching behavior; recognition of the vulva promotes the repetitive spicule thrusts as an attempt to penetrate the vulval slit; and as a result, proprioceptive signals can detect partial penetration and subsequently trigger prolonged spicule extension. The transition from one behavioral step to another is directed by one or more sensory feedback signals, and the consequential motor output is objectively purposeful and intended to obtain further sensory inputs in order to achieve the behavioral goal – vulval penetration. During this process, maintaining a precise contact with the hermaphrodite's vulva while she is moving is exceptionally challenging, as the hermaphrodite can constantly shift her direction of locomotion and can crawl on average at speeds up to ~200 μm/second [65]. Although feedback signals must be involved in these motor behaviors, sensory feedback can be delayed and can result in motor output errors. A heuristic model called the forward internal model, which potentially involves heavy computation, is proposed as a solution to this problem in motor control. A neural "controller" region generates a command to the motor unit, while simultaneously creating a copy of the command to a hypothetical region called the "forward model". The "forward model" then predicts the sensory consequences of the motor commands. The predicted sensory consequences are then compared with the actual sensory feedback in the "comparator" region, and the integrated information is sent back to the controller region to modify subsequent motor commands [66]. In neural systems of higher invertebrates and vertebrates, their complex brains can theoretically incorporate the computational components predicted in the forward internal model. However, for a simple organism like *C. elegans* that has a highly compact nervous system, we suggest that coordinating and modifying motor outputs to facilitate goal-oriented tasks can be solved by simpler, yet sufficient mechanisms.

For wild-type males, contact with the vulva and contractions of the protractor muscles take place simultaneously and rarely occur independently. This suggests that their mechanisms of execution and regulation are integrated. Efficient sensing of the vulva requires the combined functions of the bilateral set of postcloacal sensilla (p.c.s.) PCA, PCB and PCC sensory-motor neurons and the hook sensillum sensory neurons HOA and HOB. The sensory endings of the p.c.s. neurons are encased in the cuticle, suggesting that they might be mechanosensory; whereas the sensory endings of HOA and HOB neurons are opened to the environment, indicating that these neurons might sense chemical as well as mechano-signals [25]. Laser ablations of the hook sensillum cells or mutations that decrease the hook neurons' sensory functions severely reduce the ability of the male to recognize the vulva; however at low efficiency, the males can recognize the precise location of the vulva with the p.c.s. and insert their spicules [2,18,67–70]. In contrast, removal of all p.c.s. neurons results in males that can sense the general area of the vulva, but are incapable of positioning their tails over the vulval slit to insert their spicules [2,22].

Males can utilize any two of the three bilateral pairs of the p.c.s. neurons to position the cloacal opening over the vulva. But if a male lacking any single pair of the p.c.s. neurons does not quickly insert his spicules, he will move off sooner than if he had the complete sensilla. This indicates that after the initial sensory contact, the p.c.s. neurons are continually required to maintain the male's position over the vulval slit. The maintenance of the male's position over the vulva is partly regulated by direct signaling between the p.c.s. neurons and the male anterior and posterior

oblique muscles (Figure 3B, 3C; Male Wiring Project, Albert Einstein College of Medicine, http://worms.aecom.yu.edu/pages/male_wiring_project.htm). The PCB and PCC neurons are cholinergic [22]. The neurotransmitter assignment for PCA has not yet been determined, but the cell can express a reporter construct for the *eat-4* vesicular glutamate transporter, suggesting it might secrete glutamate (Garcia, unpublished observation).

Ablation of the oblique muscles or reduction in ACR-16 and UNC-29-mediated muscular cholinergic signaling causes males to behave similarly to those that have only two pairs of p.c.s. neurons. The oblique muscles are located slightly posterior to the cloacal opening, and their single sarcomeres, oriented dorsal-ventrally, are attached to the lateral body wall [25]. When they contract, the posterior tail region curls ventrally. This modification in tail curvature might redirect the force, which the male applies laterally to the hermaphrodite cuticle during backing behavior, to a downward force immediately upon vulval contact (Figure 3C). We suggest that this would stabilize the male at the vulva during his repetitive attempts to insert his spicules.

The same cells and molecules that stabilize the male at the vulva also promote the insertion of the copulatory spicules. High frequency and sustained muscle contractions of the spicule-associated muscles can be stimulated by acetylcholine (ACh) secretions from the postcloacal sensilla PCB, PCC neurons and the SPC neurons, respectively. It was hypothesized in earlier studies that the cholinergic PCB, PCC and SPC neurons differentially regulate the two types of protractor contractions via secreting different amounts or rates of ACh to activate ionotropic and muscarinic ACh receptors on the protractors [22]. The SPC neurons were known to innervate the protractors [25]. However, electron micrograph reconstruction of the male tail (Male Wiring Project) indicates that the p.c.s. neurons do not form chemical synapses to the spicule muscles. Instead, the p.c.s. neurons make multiple chemical connections to each other, to the SPC neurons and to the oblique-gubernacular muscle group (Figure 3B).

Communication between the p.c.s. neurons and the protractors are relayed through electrical junctions between the gubernacular muscles and the protractor muscles, mainly through an intermediate accessory spicule muscle called the anal depressor (Figure 3B; Male Wiring Project). In adult *C. elegans*, gap junctions are distributed extensively throughout the nervous system. Based on serial transmission electronic microscopy images and innexin expression patterns, the gap junctions are not limited between neurons or between muscles, but also connect neuron and muscle cells, where the processes penetrate the basement membrane (Male Wiring Project) [25,55,71]. These electrical connections probably play important roles in regulating animal behaviors. The worm gap junctions have been reported to mediate Ca^{2+} transient propagation throughout the intestinal cells and body wall muscles. A few studies also indicate their role in synchronizing neuron activities [49,59,72,73]. Artificially stimulating the oblique and gubernacular muscles can instantaneously induce Ca^{2+} transients and subsequent contractions in the protractor muscles. Thus, by utilizing gap junctions in the circuit, the p.c.s. neurons can coordinate both vulval contact and spicule penetration attempts simultaneously.

Although connected by gap junctions, different motor outputs are generated by the gubernacular-oblique muscle group and the protractor muscles. While males rhythmically prod their spicules at the vulva, they maintain a stable tail curvature. This suggests that the oblique muscles do not undergo high frequency contractions like the protractors. Direct p.c.s. stimulation of the oblique-gubernacular muscle group causes tonic contraction in these muscles. But signals transmitted from the oblique-gubernacular

muscle group to the spicule muscles through gap junctions facilitate rhythmic contractions of the protractors (Figure 3B, 3C). This provides a scenario that unpatterned signal input elicits patterned motor output, and this process requires intracellular regenerative Ca^{2+} transients through the UNC-68 ryanodine receptor channel [22]. The pattern generating mechanism could either be present in the protractor muscles themselves, by utilizing intracellular oscillating Ca^{2+} transients; or it can be a result of the interplay between contractions of the protractor and the retractor muscles, since the spicules are attached by both types of muscles that cause opposite directions of spicule movements.

The core spicule circuit (the p.c.s. neurons, the gubernacular-oblique muscle group, the SPC neurons, the anal depressor muscle and the spicule protractor muscles) is connected to other parts of the nervous system via extensive synapses and gap junctions (Male Wiring Project). Thus, it is likely that activity in other behavioral circuits can cause non-specific activity (noise) in the spicule circuit. Therefore, the circuit must contain contingency mechanisms to reduce the males from fully protracting their spicules into non-vulval orifices or to random environmental stimuli. The light-gated channelrhodopsin (ChR2) was used to activate different components of the core spicule circuit. Exciting cells via ChR2 is not equivalent to natural activation caused by ligand stimulation, synaptic transmission or electrical junctions in behaving animals, but these experiments provide an idea on how activated circuit components promote differential behavioral outputs.

At least three inputs must be integrated by components of the core spicule circuit for the protractors to contract completely with the highest probability via ChR2 stimulation: removal of the negative input from cells derived from the progenitor cell P10.p, possibly from the hook sensillum neurons HOA and HOB; stimulation of rhythmic contractions in the protractors via the p.c.s. sensory-motor neurons; and the addition of positive input from the SPC proprioceptive sensory-motor neurons. During mating, contact with vulval tissue would simultaneously stimulate the p.c.s. neurons and release negative regulation from the P10.p descendants. Finally, partial spicule penetration would trigger the SPC sensory-motor neurons, through their proprioceptive sensory endings, to secrete ACh onto the rhythmically contracting protractor muscles. The ACh signals from the SPC neurons could act additively with the intracellular regenerative Ca^{2+} transients to transform the oscillating contractions into a sustained one. The final motor output is the result of integrating the activities of different components in the behavioral circuit. A similar observation has been reported in other reproductive behavior systems, such as in the leech, where the oscillation frequencies of ganglia M5 and M6 are integrated to determine the rhythmic twisting behavior performed during mating [74].

We propose that the circuit uses the ERG-like K^+ channel UNC-103 to set up a high threshold for stimulating the circuit, so it responds maximally when all inputs are detected "coincidently". The "coincidence detector" mechanism collapses when UNC-103 is removed, which causes the circuit to respond to stimuli that are not normally sufficient to induce spicule protraction in normal animals. This explains why *unc-103* null mutant males spontaneously display a fictive mating behavior in the absence of hermaphrodites and prematurely protract their spicules at the hermaphrodite's vulva before they partially breach the vulval slit [60]. Similar mechanisms are used in nervous systems of other organisms. For example in vertebrates, the low excitability of the striatal neurons maintained by K^+ channels has been implied to play an important role in preventing unintended locomotion conditions [75]. The central pattern generators in the spinal cord generate the locomotion. These networks remain inhibited, until

activation of the striatum relieves this inhibition [76]. The striatum has a low excitability due to the inward rectifier K$^+$ current [77–80]. Therefore, the striatum only becomes activated when it receive strong stimulation from the thalamus or the cortex, where relevant sensory inputs are integrated. Using this mechanism, the animal adapts its locomotion properly in response to environmental conditions [75,81].

Materials and Methods

Strains

All strains were grown at 20°C on nematode growth media (NGM) plates seeded with *E. Coli* OP50 [58]. Pharmacological and behavioral assays were conducted between 21-23°C. All males contained *him-5(e1490)* on linkage group V(LGV) [82]. Additional alleles used were: *unc-29(e193)* [31,33] on LGI; *unc-103(n1213)* [83], *pha-1(e2123)* [84], *unc-64(e246)* [58] on LGIII; *acr-16(ok789)* on LGV was generated by the *C. elegans* Gene Knockout Consortium; and *unc-9(e101)* [58], *lite-1(ce314)* on LGX [85].

Behavior assays

Mating potency assay. Males were separated from hermaphrodites at the L4 stage and put onto a fresh OP50-containing NGM plate. The next day, each male was put onto an individual plate containing a "mating lawn" of OP50 with one free-moving *pha-1(e2123)* hermaphrodite. 25 µl of a saturated OP50 culture was seeded on each plate the previous night. Males and hermaphrodites were incubated together for 4 hours at 20°C, after which the males were picked off. Hermaphrodites were then incubated at 25°C, and their progeny was scored three days later. Homozygotes of *pha-1(e2123)* cannot survive beyond the L1 stage at 25°C [84]. Plates with L2 or older progeny indicated that cross fertilization occurred. The percentage of males that can sire progeny within 4 hours was recorded for each strain. To present the data, the wild-type potency was arbitrarily set to 100%, and mating potency of mutants was calculated proportional to the wild type.

Vulval contact assay. Males and hermaphrodites were separated from each other at the L4 stage, and put onto separate OP50-containing plates. The next day, 20–30 paralyzed hermaphrodites were put on a mating lawn. One male was then put onto the mating lawn and observed with a Zeiss Stemi SV 11 microscope. The male behavior was video recorded once he started scanning the hermaphrodite with his tail. Recordings were stopped 5 minutes later or when the male inserted his spicules (whichever happened first). From these videos, we quantified how long a male spent performing each step of mating behavior using a time recording Visual Basic Macro described elsewhere [26].

To determine how well a male maintains contact with the hermaphrodite's vulva, we determined the average (not cumulative) duration of vulval contact of each male. 1-day-old paralyzed *unc-64(e246)* hermaphrodites were used in this assay. The vulvas of hermaphrodites at this age were not dilated due to extended egg-laying, thus, the vast majority of the males tested in this work could not penetrate the vulva for the duration of the first vulval contact (77.3% of wild type, n = 66; 78.9% of *unc-29(lf)* locomotion-restored males, n = 19; 92.3% of *acr-16(0)* males, n = 13; 87.5% of *unc-29(lf);acr-16(0)* locomotion-restored males, n = 32; 100% of the SPC-ablated males, n = 11), and multiple vulval contacts were recorded for these males. Therefore, the average duration of vulval contact of an individual male was averaged from multiple vulval contacts, and the efficiency of spicule insertion was not likely to affect our measurements of vulval contact duration.

To present the data in figures, the average duration of vulval contact for each male was normalized to the mean of wild type or the mock-ablated males to obtain the "normalized score for vulval contact duration", as a measurement of male's ability to maintain precise vulval contact. We calculated the "normalized score for contact duration" of an individual male using: $\dfrac{x_i}{(\dfrac{\sum x_{ri}}{n_{ri}})}$ (n_{ri} is the number of males in the reference group, x_{ri} is the average duration of contract for an individual reference male (wild type or mock-ablated males), x_i is the average duration of contact for an individual male). The height of the bar represents the mean of normalized score for each strain: $\dfrac{\sum \dfrac{x_i}{(\dfrac{\sum x_{ri}}{n_{ri}})}}{n_i}$ (n_i is the number of males tested for a specific strain or treatment). Error bars indicate the standard error of the mean.

Multiple males were analyzed for each strain or treatment. Wild-type males/un-operated males were always observed in parallel with mutant males/operated males as control. Statistic comparisons were only conducted between male samples that were observed in parallel, since the wild-type behavior can vary on a day-to-day basis. Comparison between two samples was done by using the Mann-Whitney non-parametric test.

Sperm release. The behavior of males was filmed and the duration of sperm "release" was recorded as described earlier. As defined by a previous study, sperm "release" refers to the process when sperm leaves the seminal vesicle and is release from the vas deferens [20].

Measuring velocity of backward locomotion during vulva search behavior. Twenty 48 hrs adult *pha-1(e2123); him-5(e1490); lite-1(ce314);rgEx431[Phsp-16:egl-2(n693gf); Punc-103E:mDsRed; pha-1(+)]* hermaphrodites were heat shocked for 30 minutes at 30°C, and then incubated at 20°C. After 3 hrs, the heat shocked-expressed EGL-2(gf) K$^+$ channels induced complete paralysis. The hermaphrodites were placed on a 5 mm diameter lawn of *E. coli* OP50. Their postures were straightened out using an eyelash pick. 18–24 hrs adult males were then placed with the hermaphrodites and monitored at 60× total magnification on a stereomicroscope mounted with a Hamamatsu ImagEM CCD camera. Digital recordings (containing timestamps) were made at 30 frames per second. To facilitate quantification of the distances that the males moved during the vulval search behavior, images of a stage micrometer were acquired prior to recording the copulations. Velocity was determined as the time required for the male tail (focusing on the spicule tip) to travel 300 to 800 µm along the hermaphrodite's cuticle. The straight posture of the paralyzed hermaphrodites allowed easy determination of the males' position along the hermaphrodite's cuticle.

Pharmacology

Levamisole (LEV) (ICN Biomedicals, Aurora, OH) was prepared in distilled water and stored at −20°C. 400 µl of LEV solution at various concentrations was added to a Pyrex Spot Plate (nine 1 ml volume depressions), and ~5–10 virgin males were put into the drug. We observed these males for 3 minutes under a Leica MZ 7.5 stereomicroscope. A male was considered sensitive to the drug if he fully protracted his spicules for >5 seconds. Fresh drug was used after ~30 virgin males were assayed. Comparisons were made by using the Fisher's exact test.

Plasmids

Expression pattern of *unc-29*, *acr-16*, *unc-38*, *unc-63*, and *acr-18*. Primer sequences are provided in Table S1. A 5.3 kb

region upstream of the *acr-16* ATG was PCR amplified with the following primers: ATTB1acr-16 and ATTB2acr-16. A 2.4 kb region upstream of the *unc-63* ATG, plus the first three codons, was PCR amplified with the following primers: attb1unc-63 and unc-63attb2. A 4.3 kb genomic region that contained 1.2 kb upstream of the *unc-38* ATG and all *unc-38* introns and exons up to the stop codon was PCR amplified with the following primers: attb1unc-38fus and Attb2unc-38fusnew. A 2.2 kb genomic region that contained a 1.3 kb region upstream of the *unc-29* ATG and part of the *unc-29* genomic sequence up to the end of the second exon was PCR amplified with the following primers: ATTB1Punc-29 and ATTB2Punc-29. A 2.3 kb genomic region that contained 1.2 kb upstream of the *unc-29* ATG and all *unc-29* introns and exons up to the stop codon was PCR amplified with the following primers: ATTB1Punc-29 and ATTB2U29lstex. A 6.2 kb region upstream of the *acr-18* ATG was PCR amplified with the following primers: ATTB1acr-18 and ATTB2acr-18noatg. All these PCR primers contained Gateway ATTB sites, which allowed the *acr-16*, *unc-63*, *unc-38*, *unc-29* and *acr-18* PCR products to be recombined, using BP clonase (Invitrogen), into the low copy number Gateway entry vector pDG15, to generate pLR98, pLR149, pLR125, pYL21 (includes the partial *unc-29* gene), pLR198 (includes the full-length *unc-29* gene) and pLR162, respectively. In order to place the acetylcholine receptor sequences in front of YFP, pLR98, pLR149, pLR125, pYL21 and pLR198 were then individually recombined with the YFP destination vector pGW322YFP using LR clonase (Invitrogen) to make the plasmids pLR106, pLR152, pLR127, pYL22 and pLR199, respectively. pGW322YFP and pDG15 have been described in previous studies [6,44].

Cell-specific expression of the unc-29 cDNA. We inserted a SL2-accepting *trans*-splice site between the *unc-29* cDNA (including the stop codon) and the GFP gene to use GFP flourescence as a proxy for *unc-29* expression. The intergenic region between *gpd-2* and *gpd-3*, containing a SL2-accepting *trans*-splice site, was PCR amplified with the following primers: igrgpd3 and gpd2igr. This region was then cloned into the *Sma*I site of pPD95.69 (Addgene plasmid 1491) to generate pJP1. pJP1 was cut with *Hind*III and *Apa*I and then cloned into the *Hind*III/*Ava*I sites of pBR322 to generate pDG4, which contains the SL2 site in front of the GFP gene. The *unc-29* cDNA was then PCR amplified from a cDNA library using the primers Func-29 and unc-29R. The *unc-29* cDNA was cloned into the *Bam*HI site of pDG4 to generate pDG5. pDG5 was then cut with *Xba*I, blunt-ended and then ligated with the Gateway Vector Conversion Reading frame Cassette C.1 (Invitrogen) to generate pYL16. The *acr-8* and the *lev-11* promoter regions were recombined into the entry vector pDG15 to generate pLR92 and pLR22, respectively [6,34]. Then we recombined the promoter sequences in pLR92 and pLR22 into pYL16 using LR clonase (Invitrogen) to generate pYL18 and pYL20, respectively.

Cell-specific expression of ChR2. To put a Gateway destination cassette in front of ChR2, a pmyo-3::ChR2(gf)::YFP plasmid (a gift from Dr. Gottschalk, Goethe University Frankfurt) [41] was cut with *Hind*III and *Bam*HI, blunt-ended and then ligated with the Gateway Vector Conversion Reading frame Cassette C.1 (Invitrogen) to generate pZL5. A TGA stop codon 50 nucleotides downstream of the *Xba*I site was changed to GGA to generate pLR167. To express ChR2 from the promoter region of *acr-18*, *unc-103* (promoter E and F), *lev-11* and *gar-3* (promoter B), pLR162, pLR21, pLR28, pLR22 and pLR57 were subsequently recombined with pLR167 to make pLR165, pLR176, pYL41, pLR178 and pLR183, respectively. Construction of pLR21, pLR22, pLR28 and pLR57 have been described previously [5,26,34,44].

Transgenics

Plasmids were co-injected with pBX1 (50 ng/μl) into strains that contained the *pha-1(e2123)* allele. Animals that could survive beyond the L2 stage were then kept as transgenic lines. For strains that did not have the *pha-1(e2123)* allele, GFP or YFP encoded on one of the injected plasmids was used to identify transgenic animals. For all injections, pUC-18 was used to make the final concentration of DNA to 200 ng/μl. The expression constructs pLR106, pLR152, pLR127, pLR199 and pYL22 were injected at 50 ng/μl into the *pha-1(e2123); him-5(e1490); lite-1(ce314)* hermaphrodites. Multiple male-specific muscles are located within a small region of the male tail. Sometimes it was difficult to differentiate these muscles when the majority of them were expressing YFP. The expression of pLR165 (P*acr-18*:ChR2::YFP) was located on the plasma membrane and the ER, making it easier to visualize muscle expression in the male tail (Figure S3Q-S3S).

To rescue the locomotion defects of *unc-29(lf)* males, pYL18 (70 ng/μl) and pYL20 (20 ng/μl) were injected into *unc-29(e193); him-5(e1490)* or *unc-29(e193); acr-16(ok789) him-5(e1490)* hermaphrodites. To express G-CaMP and DsRed simultaneously in the male-specific muscles and express ChR2 in the oblique-gubernacular muscle group, pLR135 (20 ng/μl), pLR136 (50 ng/μl) and pLR165 (100ng/μl), were injected into the *pha-1(e2123); him-5(e1490); lite-1(ce314)* hermaphrodites. pLR35(P*unc103*E::G-CaMP) and pLR36(P*unc-103*E::DsRed) are described elsewhere [5]. To express ChR2 in specific tissues, pLR176 (50 ng/μl), pLR178 (50 ng/μl), pLR183 (100 ng/μl) and pYL41 (150 ng/μl) were injected into the *pha-1(e2123); him-5(e1490); lite-1(ce314)* hermaphrodites.

To restore functional *unc-103* to specific tissues of the *unc-103(0);Punc-103F:ChR2::YFP* worms, the P*unc-103F:unc-103F* and P*unc-103E:unc-103E* constructs [44] were injected with pYL41 (P*unc-103F:ChR2::YFP*) (150 ng/μl)into the *unc-103(0)* hermaphrodites at 20 ng/μl, respectively.

Laser ablation

Cell ablations were done using the standard protocol [86]. The operation was conducted using a Spectra-Physics VSL-337ND-S Nitrogen Laser (Mountain View, Ca) attached to an Olympus BX51 microscope. L2 worms were operated on 5% agar pads containing 0.5 mM NaN$_3$, and L4 males were operated on 5% agar pads containing 2 mM NaN$_3$. For each operated animal, a control animal was placed on the same agar pad for the same amount of time to rule out the possibility that behavioral changes are due to the anesthetic pads.

Optical stimulation and detection of repetitive spicule thrusts

lite-1(ce314) males that expressed P*acr-18*:ChR2::YFP were used. At L4 stage, males were transferred onto NGM plates with OP50 supplemented with all-*trans* retinal. Males with the same transgenes were also placed onto NGM plates with regular OP50 as control. All-*trans* retinal-containing plates were prepared the day before by spreading OP50 culture that contained 50 μM all-*trans* retinal (A.G. Scientific).

The next day, the males were immobilized on 10% agarose (in H2O) pad containing 0.5 μl of 0.1 μm diameter polystyrene microspheres, and covered with a coverglass [87]. Sequences of DIC images of the male tails were recorded under an Olympus BX51 microscope. A Dual View Simultaneous Imaging Systems by Photometrics (Surrey, BC) was used and adjusted to split the image signal, so that DIC image could be recorded in one field of view (field 1), and simultaneously, fluorescent signals could be

recorded in the other field with a dimmer DIC image (field 2) (Figure S4A, S4B). Multiple blue light pulses were applied manually to each male tested. Once the blue light was turned on, the YFP fluorescent signal was detected in field 2 and this was used to indicate the timing of light stimulation in our recording (Figure S4C). An ROI was placed in the DIC image in field 1 at the base of one spicule (Figure S4A, S4B). During spicule thrusts, light refractivity of the region defined by the ROI changed, resulting in changes in the standard deviation of the pixel intensity within this ROI (SDEV) (Figure S4C). Therefore, the value of SDEV throughout the image sequence was used to indicate the displacement of spicule.

Optical stimulation and Ca^{2+} imaging

Strains used to image Ca^{2+} transient contained *lite-1(ce314)*. Muscular Ca^{2+} transients were measured by detecting changes in fluorescence intensity of G-CaMP. The red fluorescent protein DsRed was expressed in the same set of cells as G-CaMP. Since the fluorescence intensity of DsRed does not change in response to light stimulation, it was used as an internal control. ChR2 is expressed in the gubernacular-oblique muscle group. DsRed and G-CaMP signals were recorded separately, but simultaneously via the Dual View Simultaneous Imaging Systems with an OI-11-EM filter by Photometrics (Surrey, BC). To record G-CaMP and DsRed, the transgenetic males were placed on agar pads without NaN_3, and were observed under an Olympus BX51 microscope using a $40\times$ objective. The images were recorded using a Hamamatsu ImagEM Electron multiplier (EM) CCD camera. Series of pictures were taken at the speed of $\sim$25 frames per second for 1 minute after the blue light was turned on. To record Ca^{2+} changes, each transgenic male was separated from hermaphrodites at the mid-L4 larval stage, and grown on OP50 lawns overnight. The adult male was recorded for the first time with non-functional ChR2, to obtain the baseline ratio of G-CaMP/DsRed intensity (R_0). This ratio does not change within a short period, since G-CaMP and DsRed expression were under control of the same promoter. Afterwards, they were incubated on OP50 lawns that contain all-*trans* retinal for 30 minutes and then reimaged under blue light.

Laser stimulation and Ca^{2+} imaging

Laser stimulation of muscles was slightly modified from a previous study [48]. 18–24 hr adult males containing G-CaMP and DsRed in their muscles were put on a 10% agarose (in H_2O) pad containing 0.5 µl of 0.1 µm diameter polystyrene microspheres, and covered with a coverslip [87]. The minimum output of a Spectra-Physics VSL-337ND-S Nitrogen Laser was adjusted to induce muscle contraction. The laser was aimed at the gubernaculum erector or a posterior body wall muscle, and one to ten pulses were applied to induce the muscles to contract. G-CaMP and DsRed fluorescence changes were then measured in the gubernaculum and body wall muscles, as well as the anal depressor and protractor muscles.

Analysis of Ca^{2+} imaging data

The Hamamatsu SimplePCI (version 6.6.0.0.) software was used to analyze the movies. The region-of-interest (ROI) that covers the spicule protractor and anal depressor muscles was defined manually for both G-CaMP and DsRed, and an ROI was picked far away from the male as the background region for both channels. All ROIs had the same shape and area (by using the "ROI clone" tool), and the "mean grey" of the ROIs was calculated for each frame as the fluorescence intensity. The intensity of the background region ROI was subtracted from the

sample region ROI to exclude background fluorescence from other sources.

The intensity of DsRed does not change in response to Ca^{2+} transients. The average intensity of the DsRed was calculated through the image sequence ($DsRed_{average}$). The intensity of DsRed for each frame ($DsRed_n$) deviates from the "$DsRed_{average}$" only because of photo bleaching and/or changes in muscle shape, which should contribute to G-CaMP signal change as well. To cancel out these Ca^{2+}-unrelated changes in G-CaMP signals, the intensity of G-CaMP in each frame ($G\text{-}CaMP_n$) was then normalized by using the equation of "$G\text{-}CaMP_{normalized\ n} = G\text{-}CaMP_n \times DsRed_{average}/DsRed_n$".

For the baseline recording before all-*trans* retinal incubation, a ratio of "$G\text{-}CaMP_{normalized\ n}/DsRed_{average}$" for each frame was calculated ($R_{0\ n}$), and the average of this ratio within the first 2-4 seconds of recording (R_0) was used as the baseline signal.

For the second recording after all-*trans* retinal incubation, the ratio of "$G\text{-}CaMP_{normalized\ n}/DsRed_{average}$" for each frame was also calculated (R_n). Finally, the Ca^{2+} level change ($\Delta R/R_0$) for this male was then calculated by "$(R_n - R_0)/R_0 \times 100\%$". This ratio is comparable to the $\Delta F/F0$ ratio used in other literature, except for that a G-CaMP/DsRed ratio is used instead of merely the G-CaMP intensity. The ratio $\Delta R/R_0$ was plotted over time as "corrected G-CaMP fold change trace for stimulated recording" (Figure 5B).

The maximum fold change (max. $\Delta R/R_0$) throughout the frame sequence was then calculated. Finally, the "max. $\Delta R/R_0$" was used as the maximal Ca^{2+} level change for each male, and was plotted and compared between treatments groups using the Mann-Whitney non-parametric test (Figure 5C).

Optical stimulation and continuous Ca^{2+} imaging

A demonstration unit of the Mosaic Imaging System (Andor Technology) was used to image G-CaMP and DsRed in the protractor muscles before, during and after light-stimulation of the gubernacular-oblique muscle group. The image sequences were taken at a rate of $\sim$72 frames/second. Males that expressed P*acr-18:ChR2::YFP*, P*unc-103E:G-CaMP* and P*unc-103E:DsRed* were used in this assay. Males were immobilized by using the 10% agarose pad and polystyrene microspheres described earlier. Only the region of protractors was illuminated and monitored in the first 100 frames of images ($\sim$1.4 seconds). Then, a region containing the gubernacular-oblique muscles was subsequently stimulated with blue light for 1000 frames of recording ($\sim$14 seconds). The protractors were continuously monitored during this period, and were recorded for another 500 frames ($\sim$6.9 seconds) after the end of gubernacular-oblique stimulation. The Ca^{2+} level change ($\Delta R/R_0$) was then calculated by "$(R_n - R_0)/R_0 \times 100\%$". R_n and R_0 were determined using methods described earlier. For some males, periodic spicule movements were seen before stimulation of the gubernacular muscles, due to pressure applied on the male tail by the coverglass.

RNA interference

RNAi was induced by feeding worms bacteria producing double stranded RNA to the target genes. Bacteria containing the target genes were obtained from the *C. elegans* ORF-RNAi library [88]. Bacteria with the L4440 double-T7 vector but with no target gene was used as the negative control. Bacteria were grown and induced by IPTG using a standard protocol [89]. L4 males were transferred to plates spotted with the bacteria that express dsRNA and were incubated for $\sim$20 hours. The adult males then were assayed for their response to light stimulation. The target gene

sequences in the bacteria were verified by PCR amplification and sequencing using the universal primers [88].

Injection of carbenoxolone and tubocurarine

Males that expressed P*acr-18:ChR2::YFP*, P*unc-103E:G-CaMP* and P*unc-103E:DsRed* were injected with the drugs. Carbenoxolone disodium salt (CBX) and (+)-Tubocurarine were purchased from Sigma-Aldrich (St. Louis, MO). Solution of CBX or tubocurarine was injected into the males using the same procedure as DNA microinjection. Males were imaged to obtain the baseline G-CaMP/DsRed ratio, and then were incubated on OP50 supplemented with all-*trans* retinal for 30 minutes. Drug or water was injected right after the incubation. These males were allowed to recover on OP50 supplemented with all-*trans* retinal for 1 hour, before they were imaged again to assess light-induced changes in the G-CaMP/DsRed ratio. For the injection needle not to stimulate any muscles or neurons in the male tail, one injection pulse was done at 1/3 of body length away from the posterior end of the male, the other was done in the anterior half of the male. A series of different concentrations of solution were injected for each drug to determine the proper concentration for our measurements. 7.5 mM or higher of CBX was found completely to suppress the light-induced repetitive spicule thrusts as well as the locomotion (Figure S7). Upon light stimulation, the G-CaMP signal then was measured in males that were injected with 7.5 mM CBX. The effects of different concentrations of tubocurarine were evaluated, and 7.5 mM or higher of tubocurarine was found to completely suppress the worm's locomotion. 10 mM of tubocurarine then was injected for the recordings.

Assay for blue light–induced behaviors

All strains used in this assay contained the *lite-1(ce314)* allele. At L4, males expressing the respective transgenes were transferred onto NGM plates with OP50 supplemented with all-*trans* retinal, which was prepared in the same way as described. Males with the same transgenes were also placed onto NGM plates with regular OP50 as control.

In the assay for light-induced sustained spicule protractor contraction, the SPC, PCA and PCB neurons were laser ablated in males at the mid-L4 larval stage. To remove hook associated cells, P10.p and P9.p were ablated at the L2 stage. The P*lev-11:ChR2::YFP* expressing males were assayed for light-evoked behavior on 5% agar pads without NaN$_3$. All other strains were assayed for light-evoked behavior on fresh all-*trans* retinal-supplemented OP50 plates, and their control males were assayed on standard OP50 plates. The behavior was observed using an Olympus SZX16 microscope and recorded using a Hamamatsu ImagEM Electron multiplier (EM) CCD camera. Males were illuminated with blue light from the EXFO X-Cite 120PC Q Fluorescence Illumination System, filtered with the SZX2-FGFPA GFP filter (Ex460-495/Em510-550). Males were filmed in the absence of blue light for the first few seconds and then blue light was manually turned on for ~10 seconds. Males that protracted their spicules in response to illumination for more than 5 seconds were counted as sustained spicule protraction positive.

The *unc-103(0)* males occasionally protrude their spicules in the absence of mating stimulation. Eventually, ~30% of the virgin adult males that are separated from hermaphrodites will protract their spicules permanently. We used males whose spicules were not permanently protracted for the blue light stimulation assay. To rule out the possibility that spicule protraction scored was a result of spontaneous activity of the spicule circuit instead of light-stimulated activity, only males that retracted their spicules once

the light was turned off were counted as positive for light-induced spicule protraction.

To determine the percentage of males that display rapid spicule thrusts upon blue light stimulation for the *unc-9(lf)* mutant and innexin RNAi strains, males were placed on 5% agar pads without NaN$_3$, and observed under the Olympus BX51 microscope. The blue light was manually turned on for ~5 seconds and the males that displayed repetitive spicule thrusts during this period were counted as positive.

Supporting Information

Figure S1 Velocity of backward locomotion during vulval search behavior. The velocity of locomotion during vulval search behavior was measured for wild type and locomotion-restored *unc-29(lf); acr-16(0)* males. 5 males were measured for each strain. Average velocity for each strain is marked by the red bar, and the standard deviation is also shown for each group. No significant difference was found between the two groups (p = 0.15, t test).
Found at: doi:10.1371/journal.pgen.1001326.s001 (0.19 MB TIF)

Figure S2 The raw data of average duration of vulval contact for each male tested in Figure 1 and Figure 4. (A) Profiles of the average vulval contact duration (raw data for Figure 1B). The spots represent the average vulval contact duration of individual males. The horizontal bar indicates the sample median. Each mutant strain was compared to the wild-type males using the Mann-Whitney non-parametric test. (B–D) Raw data for Figure 4A-4C. The spots represent the average vulval contact duration for each individual male. The horizontal bar indicates the sample median. Ablated males are compared to control males that mated with the same group of hermaphrodites. Data that are shown in the same panel were obtained in parallel, but cannot be compared directly to data presented in different panels. (E) Ablation of the gubernacular muscles increases the duration of sperm release (raw data for Figure 4D). The spots represent the duration of sperm release for each individual male. The horizontal bar indicates the sample median. (F) Restoring *unc-29* in male muscles reverses the vulval contact defect of the locomotion-restored *unc-29(lf); acr-16(0)* males (raw data for Figure 4E). The spots represent the average vulval contact duration of individual males. The horizontal bar indicates the sample median. Asterisks (**) indicate the *p* value <0.005, (*) indicates the *p* value <0.05, calculated using the Mann-Whitney non-parametric test.
Found at: doi:10.1371/journal.pgen.1001326.s002 (0.61 MB TIF)

Figure S3 Expression of ionotropic ACh receptor genes in the male tail. Muscle abbreviations: DSP: dorsal spicule protractor; VSP: ventral spicule protractor; DSR: dorsal spicule retractor; VSR: ventral spicule retractor; ADP: anal depressor; GER: gubernacular erector; GRT: gubernacular retractor; AOB: anterior oblique; POB: posterior oblique; SPH: sphincter. To obtain the expression pattern of *unc-29* in the *C. elegans* male, we initially fused to the YFP gene a 2.2 kb sequence, which includes a 1.3 kb of sequence upstream of the *unc-29* start codon and the genomic sequence of the gene up to the second intron (P*unc-29:YFP*). This construct is expressed in the anal depressor muscle and the spicule protractor muscles in the male spicule circuit, and it is also expressed in the body wall muscles, some ventral cord neurons and some head neurons. This is consistent with the previous published expression pattern of *unc-38*, which encodes an α-subunit that forms the L-AChR with *unc-29* (Liu *et al.* 2007). Nonetheless, the *unc-29* genomic sequence also contains important information to facilitate transcription of the gene. Therefore, the expression construct that contained the *unc-29* genomic sequence

(P*unc-29:unc-29::YFP*) provided a broader expression pattern than P*unc-29:YFP*. (A-D) Expression of P*unc-29:YFP* (yellow) and P*gar-3:CFP* (cyan) imaged from the tail of a same L4 larval male. The two images are merged to show that *unc-29* is not expressed in the SPC neurons where *gar-3* is expressing (C). The Nomarski image of the tail is also shown (D). Scale bar, 10 μm. (E, F) Expression of P*unc-29:YFP* in the male tail. Scale bar, 20 μm. We fused the 2.4 kb sequence upstream of the *unc-63* start codon, including the first three codons, to the YFP gene. We found that this construct was expressed in the body wall muscles, the sexually dimorphic anal depressor muscle and sphincter muscle, and every male-specific sex muscle, including the spicule protractor and retractor muscles, the diagonal muscles, the gubernacular muscles, and the oblique muscles. However, it was also expressed in the SPC neurons where *unc-29* was not expressed (G–J). When we made an *unc-38* promoter-genomic DNA fusion construct, we found that, similarly to *unc-63*, it was also expressed in every male-specific muscle and the SPC neurons (K–N). (G–J) Expression of P*unc-63:YFP* in the male tail. Scale bar, 10 μm. (K–N) Expression of P*unc-38:unc-38::YFP* in the male tail. Scale bar, 10 μm. (O, P) Expression of P*acr-12:acr-12::YFP* in the male tail. Scale bar, 10 μm. (Q–S) Expression of P*acr-18:ChR2::YFP* in the male tail. Scale bar, 10 μm. (T–V) Expression of P*acr-18:ChR2::YFP* (yellow) and P*pkd-2:CFP* (cyan) imaged from the tail of a same adult male. The two images are merged to show that *acr-18* is expressed in the HOA neuron that is next to the HOB neuron where *pkd-2* is expressing (V). Scale bar, 10 μm.
Found at: doi:10.1371/journal.pgen.1001326.s003 (2.78 MB TIF)

Figure S4 Brief blue light pulses induce rapid repetitive spicule thrusts (method). Red boxes depict the region of interest (ROI) and are numbered. ROI 1 is used to detect the spicule displacement, and ROI 2 is to indicate the timing of blue light stimulation. (A) A representative frame taken when the blue light was off. The pixel intensity in ROI 2 was low. (B) A representative frame taken when the blue light was on. The pixel intensity in ROI 2 was high. (C) The standard deviation of the pixel intensity within ROI 1 (SDEV) was measured and plotted as a function of time (black trace). Changes in the SDEV indicate displacement of the spicule during and between the periods of light stimulation. The green trace presents the maximal pixel intensity in ROI 2 as a function of time. The increases indicate pulses of the blue light (see Materials and Methods). The grey regions also indicate the time periods of light stimulation. Panel a, b, c and d are representative frames of field 1 taken during and between blue light pulses, and changes in refraction of the ROI 1 region are indicated. The time points when these frames were taken are indicated in the ROI 1 SDEV trace (black). a.u. arbitrary units.
Found at: doi:10.1371/journal.pgen.1001326.s004 (2.29 MB TIF)

Figure S5 Brief blue light pulses induce rapid repetitive spicule thrusts (traces of individual males). Traces represent responses of individual males to blue light pulses. The method used is described in Figure S4. Black traces indicate displacement of the spicules during and between brief blue light pulses. The green traces indicate pulses of the blue light. The grey regions also indicate the time periods of light stimulation. (A–C) Three males that expressed active P*acr-18:ChR2::YFP*, in the presence of all-*trans* retinal. (D–F) Three males that expressed inactive P*acr-18:ChR2::YFP*, in the absence of all-*trans* retinal.
Found at: doi:10.1371/journal.pgen.1001326.s005 (0.82 MB TIF)

Figure S6 Correlation between the period of incubation on all-*trans* retinal and the efficiency of light-induced behavior. To minimize possible change in the G-CaMP/DeRed intensity ratio during incubation with all-*trans* retinal, we determined the minimal period of incubation that is sufficient to elicit ChR2-induced

behavior. We used males that expressed P*gar-3b:ChR2::YFP* and males that expressed P*acr-18:ChR2::YFP*. We allowed these males to be incubated on the all-*trans* retinal-containing plates for 0 min, 15 min, 30 min, 60 min and overnight. We then determined the percentage of the male population that protracted their spicules upon blue light stimulation for the P*gar-3b:ChR2::YFP* males (upper panel), and determined the percentage of the male population that displayed rapid spicule thrusts upon light stimulation for males that expressed P*acr-18:ChR2::YFP* (lower panel). We found in both cases, 30 min of incubation was sufficient to induce ChR2-elicited behavior and the efficiency was not significantly different from overnight incubation. The number of males assayed for each strain is listed within each bar (for 0 min, the number is above the X-axis). The number above the bar refers to the percentage of males displayed light-induced behavior. Asterisk (*) indicates the *p* value <0.05, (**) indicate the *p* value <0.001, (***) indicate the *p* value <0.0001, using the Fisher's exact test.
Found at: doi:10.1371/journal.pgen.1001326.s006 (0.52 MB TIF)

Figure S7 Carbenoxolone inhibition of blue light-induced repetitive spicule thrusts. CBX was injected at the concentration of 1 mM, 2.5 mM, 5 mM, 7.5 mM and 10 mM, to differentially suppress light-induced repetitive spicule thrusts in males that express P*acr-18:ChR2::YFP*, P*unc-103E:G-CaMP* and P*unc-103E:DsRed*. ~10 males were assayed at each concentration. The X-axis plots concentration of the CBX, and the Y-axis plots the percentage of males that still displayed light-induced spicule thrusts. A log(agonist) vs. Normalized response-variable slope curve is fit to the data to estimate the minimal concentration of CBX that can inhibit light-induced spicule thrusts in the majority of the males.
Found at: doi:10.1371/journal.pgen.1001326.s007 (0.14 MB TIF)

Figure S8 Male tail expression of *unc-9* and *inx-14*. Muscle abbreviations: DSP: dorsal spicule protractor; ADP: anal depressor; GER: gubernacular erector; GRT: gubernacular retractor; AOB: anterior oblique; POB: posterior oblique. (A-H) Expression of *unc-9* in the adult male tail (B, D, F and H), and the corresponding DIC images of the male tail (A, C, E and G, respectively). (I-N) Expression of *inx-14* in the adult male tail (J, L and N), and the corresponding DIC images of the male tail (I, K and M, respectively). All images were taken at 100×. Scale bar, 20 μm. The expression pattern was obtained by using transcriptional GFP fusion constructs (Altun *et al.* 2009) [55].
Found at: doi:10.1371/journal.pgen.1001326.s008 (2.05 MB TIF)

Table S1 Primers used in this study.
Found at: doi:10.1371/journal.pgen.1001326.s009 (0.03 MB DOC)

Video S1 In the presence of all-*trans* retinal, brief blue light pulses induce corresponding rapid repetitive spicule thrusts in a male that expresses ChR2 in the gubernacular-oblique muscle group.
Found at: doi:10.1371/journal.pgen.1001326.s010 (5.17 MB WMV)

Video S2 In the absence of all-*trans* retinal, a male that expresses ChR2 in the gubernacular-oblique muscle group does not respond to blue light pulses.
Found at: doi:10.1371/journal.pgen.1001326.s011 (4.16 MB WMV)

Video S3 In the presence of all-*trans* retinal, Ca^{2+} transients are induced in the spicule protractors under blue light when ChR2 is expressed on the gubernacular-oblique muscle group.
Found at: doi:10.1371/journal.pgen.1001326.s012 (0.76 MB WMV)

Video S4 In the absence of all-*trans* retinal, no Ca^{2+} transient is induced under the blue light when ChR2 is expressed.
Found at: doi:10.1371/journal.pgen.1001326.s013 (1.71 MB WMV)

Video S5 Optical stimulation of the gubernacular-oblique muscles, which express ChR2, elicits Ca^{2+} transients in the spicule protractors in the presence of all-*trans* retinal.
Found at: doi:10.1371/journal.pgen.1001326.s014 (0.83 MB WMV)

Video S6 Optical stimulation of the gubernacular-oblique muscles, which express ChR2, does not elicit Ca^{2+} transients in the spicule protractors in the absence of all-*trans* retinal.
Found at: doi:10.1371/journal.pgen.1001326.s015 (0.53 MB WMV)

Video S7 Laser stimulation of the gubernacular erector induces Ca^{2+} transients in the spicule protractor-anal depressor muscles.
Found at: doi:10.1371/journal.pgen.1001326.s016 (4.91 MB WMV)

Video S8 Laser stimulation of a body wall muscle does not induce Ca^{2+} transients in the spicule protractor-anal depressor muscles.
Found at: doi:10.1371/journal.pgen.1001326.s017 (6.48 MB WMV)

Video S9 Light-induced behavior of a male expressing P*lev-11:ChR2::YFP*.
Found at: doi:10.1371/journal.pgen.1001326.s018 (3.26 MB WMV)

Video S10 Light-induced behavior of a male expressing P*unc-103E:ChR2::YFP*.
Found at: doi:10.1371/journal.pgen.1001326.s019 (4.75 MB WMV)

Video S11 Light-induced behavior of a male expressing P*gar-3B:ChR2::YFP*.
Found at: doi:10.1371/journal.pgen.1001326.s020 (1.36 MB WMV)

Author Contributions

Conceived and designed the experiments: YL LRG. Performed the experiments: YL BL XG PAC DGG LRG. Analyzed the data: YL BL XG LRG. Contributed reagents/materials/analysis tools: YL RL LRG. Wrote the paper: YL LRG.

References

1. Emmons SW, Lipton J (2003) Genetic basis of male sexual behavior. J Neurobiol 54: 93–110.
2. Liu KS, Sternberg PW (1995) Sensory regulation of male mating behavior in *Caenorhabditis elegans*. Neuron 14: 79–89.
3. de Bono M, Maricq AV (2005) Neuronal substrates of complex behaviors in *C. elegans*. Annu Rev Neurosci 28: 451–501.
4. Lipton J, Kleemann G, Ghosh R, Lints R, Emmons SW (2004) Mate searching in *Caenorhabditis elegans*: a genetic model for sex drive in a simple invertebrate. J Neurosci 24: 7427–7434.
5. Gruninger TR, Gualberto DG, Garcia LR (2008) Sensory perception of food and insulin-like signals influence seizure susceptibility. PLoS Genet 4: e1000117. doi:10.1371/journal.pgen.1000117.
6. Gruninger TR, Gualberto DG, LeBoeuf B, Garcia LR (2006) Integration of male mating and feeding behaviors in *Caenorhabditis elegans*. J Neurosci 26: 169–179.
7. Lee K, Portman DS (2007) Neural sex modifies the function of a *C. elegans* sensory circuit. Curr Biol 17: 1858–1863.
8. Sengupta P, Samuel AD (2009) *Caenorhabditis elegans:* a model system for systems neuroscience. Curr Opin Neurobiol 19: 637–643.
9. Sokolowski MB (2010) Social interactions in "simple" model systems. Neuron 65: 780–794.
10. Barr MM, Garcia LR (2006) Male mating behavior WormBook, ed The *C elegans* Research Community, WormBook, doi/101895/wormbook1781 http://wwwwormbookorg.
11. Schafer WF (2006) Genetics of egg-laying in worms. Annu Rev Genet 40: 487–509.
12. Branicky R, Hekimi S (2006) What keeps *C. elegans* regular: the genetics of defecation. Trends Genet 22: 571–579.
13. Rankin CH (2006) Nematode behavior: the taste of success, the smell of danger! Curr Biol 16: R89–91.
14. Bargmann CI (2006) Chemosensation in C. elegans WormBook, ed The *C elegans* Research Community, WormBook, doi/101895/wormbook11231, http://wwwwormbookorg.
15. Goodman MB (2006) Mechanosensation WormBook, ed The *C elegans* Research Community, WormBook, http://wwwwormbookorg January 06.
16. Mori I, Sasakura H, Kuhara A (2007) Worm thermotaxis: a model system for analyzing thermosensation and neural plasticity. Curr Opin Neurobiol 17: 712–719.
17. Zhang M, Chung SH, Fang-Yen C, Craig C, Kerr RA, et al. (2008) A self-regulating feed-forward circuit controlling *C. elegans* egg-laying behavior. Curr Biol 18: 1445–1455.
18. Barr MM, Sternberg PW (1999) A polycystic kidney-disease gene homologue required for male mating behaviour in C. elegans. Nature 401: 386–389.
19. Liu T, Kim K, Li C, Barr M (2007) FMRFamide-like neuropeptides and mechanosensory touch receptor neurons regulate male sexual turning behavior in *Caenorhabditis elegans*. J Neurosci 27: 7174–7182.
20. Schindelman G, Whittaker AJ, Thum JY, Gharib S, Sternberg PW (2006) Initiation of male sperm-transfer behavior in *Caenorhabditis elegans* requires input from the ventral nerve cord. BMC Biol 4: 26.
21. Whittaker A, Sternberg P (2009) Coordination of opposing sex-specific and core muscle groups regulates male tail posture during *Caenorhabditis elegans* male mating behavior. BMC Biol 7: 33.
22. Garcia LR, Mehta P, Sternberg PW (2001) Regulation of distinct muscle behaviors controls the *C. elegans* male's copulatory spicules during mating. Cell 107: 777–788.
23. Kleemann GA, Basolo AL (2007) Facultative decrease in mating resistance in hermaphroditic *Caenorhabditis elegans* with self-sperm depletion. Animal Behaviour 74: 1337–1347.
24. Garcia LR, LeBoeuf B, Koo P (2007) Diversity in mating behavior of hermaphroditic and male-female Caenorhabditis nematodes. Genetics 175: 1761–1771.
25. Sulston JE, Albertson DG, Thomson JN (1980) The *Caenorhabditis elegans* male: postembryonic development of nongonadal structures. Dev Biol 78: 542–576.
26. Liu Y, LeBoeuf B, Garcia LR (2007) G alpha(q)-coupled muscarinic acetylcholine receptors enhance nicotinic acetylcholine receptor signaling in *Caenorhabditis elegans* mating behavior. J Neurosci 27: 1411–1421.
27. Fleming JT, Squire MD, Barnes TM, Tornoe C, Matsuda K, et al. (1997) *Caenorhabditis elegans* levamisole resistance genes *lev-1, unc-29, and unc-38* encode functional nicotinic acetylcholine receptor subunits. J Neurosci 17: 5843–5857.
28. Rayes D, Flamini M, Hernando G, Bouzat C (2007) Activation of single nicotinic receptor channels from *Caenorhabditis elegans* muscle. Mol Pharmacol 71: 1407–1415.
29. Richmond JE, Jorgensen EM (1999) One GABA and two acetylcholine receptors function at the *C. elegans* neuromuscular junction. Nat Neurosci 2: 791–797.
30. Ballivet M, Alliod C, Bertrand S, Bertrand D (1996) Nicotinic acetylcholine receptors in the nematode *Caenorhabditis elegans*. J Mol Biol 258: 261–269.
31. Lewis JA, Wu CH, Berg H, Levine JH (1980) The genetics of levamisole resistance in the nematode *Caenorhabditis elegans*. Genetics 95: 905–928.
32. Kim J, Poole DS, Waggoner LE, Kempf A, Ramirez DS, et al. (2001) Genes affecting the activity of nicotinic receptors involved in *Caenorhabditis elegans* egg-laying behavior. Genetics 157: 1599–1610.
33. Lewis JA, Wu CH, Levine JH, Berg H (1980) Levamisole-resistant mutants of the nematode *Caenorhabditis elegans* appear to lack pharmacological acetylcholine receptors. Neuroscience 5: 967–989.
34. LeBoeuf B, Gruninger TR, Garcia LR (2007) Food deprivation attenuates seizures through CaMKII and EAG K+ channels. PLoS Genet 3: e156. doi:10.1371/journal.pgen.0030156.
35. Touroutine D, Fox RM, Von Stetina SE, Burdina A, Miller DM, 3rd, et al. (2005) acr-16 encodes an essential subunit of the levamisole-resistant nicotinic receptor at the *Caenorhabditis elegans* neuromuscular junction. J Biol Chem 280: 27013–27021.
36. Jospin M, Qi YB, Stawicki TM, Boulin T, Schuske KR, et al. (2009) A neuronal acetylcholine receptor regulates the balance of muscle excitation and inhibition in *Caenorhabditis elegans*. PLoS Biol 7: e1000265. doi:10.1371/journal.pbio.1000265.

37. Lints R, Hall DH (2009) Male muscle system, male-specific muscles. In *WormAtlas* doi:103908/wormatlas25.

38. Gower NJ, Walker DS, Baylis HA (2005) Inositol 1,4,5-trisphosphate signaling regulates mating behavior in *Caenorhabditis elegans* males. Mol Biol Cell 16: 3978–3986.

39. Bennett MV, Zukin RS (2004) Electrical coupling and neuronal synchronization in the Mammalian brain. Neuron 41: 495–511.

40. Bennett MV, Barrio LC, Bargiello TA, Spray DC, Hertzberg E, et al. (1991) Gap junctions: new tools, new answers, new questions. Neuron 6: 305–320.

41. Nagel G, Brauner M, Liewald JF, Adeishvili N, Bamberg E, et al. (2005) Light activation of channelrhodopsin-2 in excitable cells of *Caenorhabditis elegans* triggers rapid behavioral responses. Curr Biol 15: 2279–2284.

42. Nagel G, Szellas T, Huhn W, Kateriya S, Adeishvili N, et al. (2003) Channelrhodopsin-2, a directly light-gated cation-selective membrane channel. Proc Natl Acad Sci U S A 100: 13940–13945.

43. Nakai J, Ohkura M, Imoto K (2001) A high signal-to-noise Ca(2+) probe composed of a single green fluorescent protein. Nat Biotechnol 19: 137–141.

44. Reiner DJ, Weinshenker D, Tian H, Thomas JH, Nishiwaki K, et al. (2006) Behavioral genetics of *caenorhabditis elegans unc-103*-encoded erg-like K(+) channel. J Neurogenet 20: 41–66.

45. Matz MV, Fradkov AF, Labas YA, Savitsky AP, Zaraisky AG, et al. (1999) Fluorescent proteins from nonbioluminescent Anthozoa species. Nat Biotechnol 17: 969–973.

46. Baird GS, Zacharias DA, Tsien RY (2000) Biochemistry, mutagenesis, and oligomerization of DsRed, a red fluorescent protein from coral. Proc Natl Acad Sci U S A 97: 11984–11989.

47. Zhang F, Prigge M, Beyriere F, Tsunoda SP, Mattis J, et al. (2008) Red-shifted optogenetic excitation: a tool for fast neural control derived from Volvox carteri. Nat Neurosci 11: 631–633.

48. Reiner DJ, Weinshenker D, Thomas JH (1995) Analysis of dominant mutations affecting muscle excitation in *Caenorhabditis elegans*. Genetics 141: 961–976.

49. Peters MA, Teramoto T, White JQ, Iwasaki K, Jorgensen EM (2007) A calcium wave mediated by gap junctions coordinates a rhythmic behavior in *C. elegans*. Curr Biol 17: 1601–1608.

50. Davidson JS, Baumgarten IM (1988) Glycyrrhetinic acid derivatives: a novel class of inhibitors of gap-junctional intercellular communication. Structure-activity relationships. J Pharmacol Exp Ther 246: 1104–1107.

51. Schneider NL, Stengl M (2006) Gap junctions between accessory medulla neurons appear to synchronize circadian clock cells of the cockroach Leucophaea maderae. J Neurophysiol 95: 1996–2002.

52. Bao L, Samuels S, Locovei S, Macagno ER, Muller KJ, et al. (2007) Innexins form two types of channels. FEBS Lett 581: 5703–5708.

53. Raizen DM, Lee RY, Avery L (1995) Interacting genes required for pharyngeal excitation by motor neuron MC in *Caenorhabditis elegans*. Genetics 141: 1365–1382.

54. Sattelle DB, Culetto E, Grauso M, Raymond V, Franks CJ, et al. (2002) Functional genomics of ionotropic acetylcholine receptors in *Caenorhabditis elegans* and *Drosophila melanogaster*. Novartis Found Symp 245: 240–257; discussion 257-260, 261-244.

55. Altun ZF, Chen B, Wang ZW, Hall DH (2009) High resolution map of *Caenorhabditis elegans* gap junction proteins. Dev Dyn 238: 1936–1950.

56. Starich T, Sheehan M, Jadrich J, Shaw J (2001) Innexins in *C. elegans*. Cell Commun Adhes 8: 311–314.

57. Sulston JE, Horvitz HR (1977) Post-embryonic cell lineages of the nematode, *Caenorhabditis elegans*. Dev Biol 56: 110–156.

58. Brenner S (1974) The genetics of *Caenorhabditis elegans*. Genetics 77: 71–94.

59. Liu Q, Chen B, Gaier E, Joshi J, Wang ZW (2006) Low conductance gap junctions mediate specific electrical coupling in body-wall muscle cells of *Caenorhabditis elegans*. J Biol Chem 281: 7881–7889.

60. Garcia LR, Sternberg PW (2003) *Caenorhabditis elegans* UNC-103 ERG-like potassium channel regulates contractile behaviors of sex muscles in males before and during mating. J Neurosci 23: 2696–2705.

61. Franks CJ, Murray C, Ogden D, O'Connor V, Holden-Dye L (2009) A comparison of electrically evoked and channel rhodopsin-evoked postsynaptic potentials in the pharyngeal system of *Caenorhabditis elegans*. Invert Neurosci 9: 43–56.

62. Baier H, Scott EK (2009) Genetic and optical targeting of neural circuits and behavior—zebrafish in the spotlight. Curr Opin Neurobiol 19: 553–560.

63. Guo ZV, Hart AC, Ramanathan S (2009) Optical interrogation of neural circuits in *Caenorhabditis elegans*. Nat Methods 6: 891–896.

64. Schroeder CE, Wilson DA, Radman T, Scharfman H, Lakatos P (2010) Dynamics of Active Sensing and perceptual selection. Curr Opin Neurobiol 20: 172–176.

65. Cronin CJ, Mendel JE, Mukhtar S, Kim YM, Stirbl RC, et al. (2005) An automated system for measuring parameters of nematode sinusoidal movement. BMC Genet 6: 5.

66. Shadmehr R, Smith MA, Krakauer JW (2010) Error correction, sensory prediction, and adaptation in motor control. Annu Rev Neurosci 33: 89–108.

67. Yu H, Pretot R, Burglin T, Sternberg P (2003) Distinct roles of transcription factors EGL-46 and DAF-19 in specifying the functionality of a polycystin-expressing sensory neuron necessary for *C. elegans* male vulva location behavior. Development 130: 5217–5227.

68. Peden E, Barr M (2005) The KLP-6 kinesin is required for male mating behaviors and polycystin localization in *Caenorhabditis elegans*. Curr Biol 15: 394–404.

69. Jauregui A, Barr M (2005) Functional characterization of the *C. elegans* nephrocystins NPHP-1 and NPHP-4 and their role in cilia and male sensory behaviors. Exp Cell Res 305: 333–342.

70. Bae Y-K, Lyman-Gingerich J, Barr M, Knobel K (2008) Identification of genes involved in the ciliary trafficking of *C. elegans* PKD-2. Developmental Dynamics 237: 2021–2029.

71. White JG, Southgate E, Thomson JN, Brenner S (1986) The Structure of the Nervous System of the Nematode *Caenorhabditis elegans*. Phil Trans Royal Soc London Series B, Biol Scien 314: 1–340.

72. Macosko EZ, Pokala N, Feinberg EH, Chalasani SH, Butcher RA, et al. (2009) A hub-and-spoke circuit drives pheromone attraction and social behaviour in *C. elegans*. Nature 458: 1171–1175.

73. Chen B, Liu Q, Ge Q, Xie J, Wang ZW (2007) UNC-1 regulates gap junctions important to locomotion in *C. elegans*. Curr Biol 17: 1334–1339.

74. Wagenaar DA, Hamilton MS, Huang T, Kristan WB, French KA (2010) A hormone-activated central pattern generator for courtship. Curr Biol 20: 487–495.

75. Grillner S, Wallen P, Saitoh K, Kozlov A, Robertson B (2008) Neural bases of goal-directed locomotion in vertebrates—an overview. Brain Res Rev 57: 2–12.

76. Grillner S, Jessell TM (2009) Measured motion: searching for simplicity in spinal locomotor networks. Curr Opin Neurobiol 19: 572–586.

77. Nisenbaum ES, Wilson CJ (1995) Potassium currents responsible for inward and outward rectification in rat neostriatal spiny projection neurons. J Neurosci 15: 4449–4463.

78. Kreitzer AC, Malenka RC (2008) Striatal plasticity and basal ganglia circuit function. Neuron 60: 543–554.

79. Mermelstein PG, Song WJ, Tkatch T, Yan Z, Surmeier DJ (1998) Inwardly rectifying potassium (IRK) currents are correlated with IRK subunit expression in rat nucleus accumbens medium spiny neurons. J Neurosci 18: 6650–6661.

80. Wilson CJ, Kawaguchi Y (1996) The origins of two-state spontaneous membrane potential fluctuations of neostriatal spiny neurons. J Neurosci 16: 2397–2410.

81. Grillner S, Hellgren J, Menard A, Saitoh K, Wikstrom MA (2005) Mechanisms for selection of basic motor programs—roles for the striatum and pallidum. Trends Neurosci 28: 364–370.

82. Hodgkin JA, Horvitz HR, Brenner S (1979) Nondisjunction mutants of the nematode *Caenorhabditis elegans*. Genetics 91: 67–94.

83. Park EC, Horvitz HR (1986) Mutations with dominant effects on the behavior and morphology of the nematode *Caenorhabditis elegans*. Genetics 113: 821–852.

84. Schnabel H, Schnabel R (1990) An Organ-Specific Differentiation Gene, *pha-1*, from *Caenorhabditis elegans*. Science 250: 686–688.

85. Edwards S, Charlie N, Milfort M, Brown B, Gravlin C, et al. (2008) A novel molecular solution for ultraviolet light detection in *Caenorhabditis elegans*. PLoS Biol 6: e198. doi:10.1371/journal.pbio.0060198.

86. Bargmann CI, Avery L (1995) Laser killing of cells in *Caenorhabditis elegans*. Methods Cell Biol 48: 225–250.

87. Fang-Yen C, Wasserman S, Sengupta P, Samuel AD (2009) Agarose immobilization of *C. elegans*. Worm Breeder's Gazette 18: 32.

88. Rual JF, Ceron J, Koreth J, Hao T, Nicot AS, et al. (2004) Toward improving *Caenorhabditis elegans* phenome mapping with an ORFeome-based RNAi library. Genome Res 14: 2162–2168.

89. Kamath RS, Martinez-Campos M, Zipperlen P, Fraser AG, Ahringer J (2001) Effectiveness of specific RNA-mediated interference through ingested double-stranded RNA in *Caenorhabditis elegans*. Genome Biol 2: RESEARCH0002.